RANGE OF AND RELATIONSHIPS BETWEEN PHYSICAL AND HYDRAULIC PROPERTIES OF COMMONLY AVAILABLE DENITRIFYING BIOREACTOR WOODCHIPS

BY

GABRIEL MATTHEW JOHNSON

THESIS

Submitted in partial fulfillment of the requirements
for the degree of Master of Science in Agricultural and Biological Engineering
in the Graduate College of the
University of Illinois Urbana-Champaign, 2021

Urbana, Illinois

Advisers:

Assistant Professor Laura E. Christianson, Chair
Research Assistant Professor Reid D. Christianson
Professor Richard A. C. Cooke

ABSTRACT

Saturated hydraulic conductivity (K_{sat}), porosity, and particle size are key physical parameters of woodchip media for denitrifying bioreactor design. Current design guidelines can be improved by analyzing more woodchip types and the effects of overburden on woodchip properties. The objectives of this study were to quantify and determine the relationships between K_{sat}, porosity, particle size, and bulk density of 21 woodchip types from the United States Midwest region to improve bioreactor design specifications. Saturated hydraulic conductivity was estimated using constant head permeameters and Darcy's Law assumptions. Drainable porosity was assessed both by packing 1 L beakers ("jar method") and in the permeameters. Particle size analysis was performed using a sieve shaker, as well as by manually measuring the longest, middle, and shortest axis of individual woodchip particles with a caliper. High compaction methods limited the range and magnitude of K_{sat} for 20 typical woodchip types to 0.10 to 2.05 cm s^{-1}. Reduced compaction increased K_{sat} and drainable porosity for a subset of woodchips to values closer to current practice standards (2.07 to 7.44 cm s^{-1} and 41 to 55%, respectively). Drainable porosity (permeameter method) and hand-measured woodchip median width were the only significant predictors of K_{sat} in a multiple linear regression model (K_{sat} = $0.081*DP_{perm} + 0.048*W_{med}$; $R^2 = 0.48$), however the model was limited by the small range in K_{sat} values resulting from high compaction. These results can inform bioreactor design specifications but better guidance can be provided by contextualizing these results with *in situ* bulk density measurements which are suggested as future research.

ACKNOWLEDGMENTS

I would like to thank everyone who has supported me over these last two years. First, thank you to my advisor Dr. Laura Christianson who has pushed me to continually improve both as a student and researcher, and encouraged me through the various challenges I faced along the way, from experimental design troubleshooting to continuing my research during a pandemic. Additionally, thank you to my two other committee members, Dr. Reid Christianson and Dr. Richard Cooke, for their assistance with my experimental design, their incredibly valuable comments to improve this thesis, and their positive encouragement throughout my studies.

This work would not have been possible without the support of our funders, partners, and collaborators. Specifically, this study was funded by project NR185A12XXXXC004 CESU under the Great Rivers Umbrella Agreement 68-3A75-18-504 (USDA-NRCS). We would also like to acknowledge two private farmers in Illinois with new bioreactors and the Illinois Farm Bureau Bioreactor Partnership. Lastly, we would like to thank the Illinois Nutrient Research and Education Council project: Bioreactors for Illinois: Smaller, Better, Faster (NREC 2017-4-360498-302) as some woodchips from that project were studied here.

This study was a team effort with many of my I-DROP colleagues assisting me. Specific thanks to Annie Brunton, Ronnie Chacon, Charles Dochoff, Molly Duncan, and Ariana Munoz Ventura for their help with woodchip collection, experimental runs, and CAD drawings.

Finally, thank you to my friends and family who have provided encouragement and inspiration and helped me endeavor through this project.

To Grandpa and Grandma Obermann

TABLE OF CONTENTS

CHAPTER 1: INTRODUCTION

Conventional agricultural systems in the United States Midwest region use inorganic nitrogen fertilizer and artificial subsurface drainage improvements to produce high crop yields. While these subsurface drainage ("tile drainage") systems increase field trafficability and reduce crop yield losses from wet conditions, they also export nutrients directly from the field into waterways (Dinnes et al., 2002). Nitrate-nitrogen (NO_3-N) from fertilizer applications and naturally present in the soil can leach into drainage water resulting in elevated nitrate concentrations in downstream rivers and lakes. This nitrate can impair water quality by inducing excessive algae growth that causes eutrophic and hypoxic conditions and can negatively impact human health by contaminating drinking water supplies (Blowes et al., 1994). Elevated nitrate concentrations in Mississippi River discharge, largely attributed to runoff and drainage from agricultural lands, are a major contributing factor to the annual "dead zone", a region of intense hypoxia, in the Gulf of Mexico (Rabalais et al., 1996; Rabalais et al., 2002). To address this issue, the Mississippi River/Gulf of Mexico Watershed Nutrient Task Force developed an action plan that called for implementation of strategies to reduce nutrient losses (Mississippi River/Gulf of Mexico Watershed Nutrient Task Force, 2001).

Denitrifying bioreactors are one of several practices developed to reduce nitrate losses from agricultural lands. These bioreactors specifically address nitrate loss from tile drainage by intercepting drainage water before it discharges into streams. Denitrifying bioreactors function by diverting drainage water through a trench filled with carbon media, usually woodchips, which serves as an energy source for denitrifying bacteria. Denitrifying bacteria convert the nitrate into inert nitrogen (N_2) gas (Blowes et al., 1994; Christianson et al., 2010; van Driel et al., 2006). A key bioreactor design parameter is the hydraulic retention time (HRT), the amount of time it

takes water to completely flow through the bioreactor (Christianson et al., 2010; Christianson et al., 2012). The longer the HRT, the longer the time for the bacteria to convert the nitrate to nitrogen gas. Current practice standards call for bioreactor HRT to be at least three hours and that the bioreactor be designed to reduce nitrate by 20% considering untreated bypass flow (USDA-NRCS, 2020). However, this depends upon accurate knowledge of the bioreactor flow regime which is affected by the physical properties of the carbon media, including particle size, porosity, bulk density, and saturated hydraulic conductivity (K_{sat}) (Cameron and Schipper, 2012; Christianson et al., 2010; Feyereisen and Christianson, 2015).

Woodchips are the most commonly used carbon media due to their longevity, hydraulic and denitrification performance, accessibility, and cost (Christianson et al., 2010; Cooke et al., 2001; Greenan et al., 2006; Schipper et al., 2010). Current practice standards suggest using woodchips 25 to 50 mm in effective diameter with limited amounts of sawdust or fines (USDA-NRCS, 2020). While the NRCS standard does not specify design values for porosity and K_{sat}, Illinois NRCS uses porosities ranging from 47 to 64% depending on woodchip type (hardwood, shredded, or mixed) and overburden (soil cover), with default design values of 53% and 2.94 cm s^{-1} provided in the Illinois NRCS Denitrifying Bioreactor Design Spreadsheet (Illinois NRCS, 2021; USDA-NRCS, 2019). These recommendations were based on work by van Driel et al. (2006), Chun et al. (2009), and Cooke and Bell (2014) who reported porosity and K_{sat} values ranging from 39 to 88% and 0.12 to 4.9 cm s^{-1}, respectively, for mixed wood media ranging in size from fine sawdust to 50 mm woodchips. Cooke and Bell (2014) measured drainable porosity in laboratory columns under three levels of overburden that simulated field conditions of soil overburden. They found porosity decreased by 4, 4, and 6% for hardwood, shredded, and mixed woodchips, respectively, from adding an overburden pressure similar to 30.5 cm of soil in the

field, but porosity was different by 1% or less from 61 cm of soil overburden to 30.5 cm of soil overburden.

Other studies have found similar values for porosity but a variety of K_{sat} values. Christianson et al. (2010) reported a mean K_{sat} of 9.50 cm s^{-1} and porosity ranging from 66 to 78% for mixed woodchips at a bulk density of 290 kg m^{-3} (oven-dry) and an effective size of 6.5 mm. However, later work by Feyereisen and Christianson (2015) suggested the K_{sat} was initially overestimated due to non-linear effects and was corrected to 5.54 cm s^{-1}. Feyereisen and Christianson (2015) also used non-linear methods and reported mean K_{sat} and drainable porosity of 4.47 cm s^{-1} and 46%, respectively, for mixed woodchips at a dry bulk density of 220 kg m^{-3} and approximately 10 mm in median size. They also noted that non-linearity may need to be considered when comparing results of prior studies. Non-linear methods were specifically used in studies by Ghane, Fausey, and Brown (2014) and Ghane, Feyereisen, and Rosen (2016) resulting in K_{sat} values ranging from 2.2 to 11.1 cm s^{-1} for both fresh and aged woodchips 7.6 to 9.1 mm in median size in both field and laboratory tests. Some of the highest K_{sat} values for wood media were documented by Burbery et al. (2014) who found values of 12.2 and 10.1 cm s^{-1} for chipped and "hogged" (shredded) wood 17 mm in length, and 31.2 cm s^{-1} for "hogged" wood 77 mm in length. However, the drainable porosities of the 17 mm chipped, 17 mm hogged, and 77 mm hogged media were 43, 45, and 47%, respectively, similar to other studies with lower values of K_{sat}. Cameron and Schipper (2010) also reported relatively high K_{sat} values ranging from 6.4 to 11.6 cm s^{-1} for 61 mm woodchips with a drainable porosity of 56% at a bulk density of 177 kg m^{-3}.

Despite a seeming consensus for some woodchip properties (e.g., design values used by Illinois NRCS), there remains a need to investigate more types of woodchips that may not meet

standard specifications (e.g., woodchips from farm storm debris) and investigate the effects of woodchip compaction on physical properties. Additionally, analyzing the relationships between woodchip physical and hydraulic properties could enable estimation of properties that are laborious to measure (i.e. K_{sat}) from easier-to-measure properties (i.e. particle size).

The objectives of this study were to quantify and develop relationships between particle size, porosity, bulk density, and saturated hydraulic conductivity of 21 woodchip types to improve understanding of the range and sensitivity of these properties from woodchips commonly available across the US Midwest. A secondary objective was to investigate the effects of woodchip compression on these properties as a simulation of overburden in field bioreactors. There were three main hypotheses: (1) K_{sat} would vary across woodchip types and be positively correlated with particle size and drainable porosity, but negatively correlated with bulk density; (2) average drainable porosity would be similar to prior studies (near 50%) but would depend on bulk density; and (3) manual length, width, and depth particle size measurements may be more strongly associated with K_{sat} than sieve measurements due to the oblong nature of many woodchips. The results of this study were intended to inform values used for physical and hydraulic properties in denitrifying bioreactor design models. Ultimately, better knowledge of woodchip media properties and their relationships can provide conservation professionals and landowners the ability to use different types of woodchips in denitrifying bioreactors, reducing a barrier to adoption of bioreactors throughout the Midwest which would eventually improve water quality.

CHAPTER 2: METHODS

2.1 WOODCHIP COLLECTION

Twenty-one woodchip types were collected from lawn and garden stores, composting facilities, bulk woodchip suppliers, and bioreactor installations across Illinois, Iowa, and Michigan between September 2019 and December 2020 (Figure 1; Table 1). Approximately 100 to 130 L of each woodchip type was collected based on the required volume for the variety of tests performed which were generally done in triplicate. Woodchips were air-dried and stored in closed plastic tubs until testing in the Illinois Drainage Research and Outreach Program (I-DROP) laboratory at the University of Illinois Urbana-Champaign (mean 20 ± 0.3°C, 62 ± 4% relative humidity).

Figure 1. Photo illustration of twenty-one woodchip types commonly available in the Midwest (IL, IA, MI) evaluated for physical and hydraulic properties.

Table 1. Twenty-one commercially available woodchips from across Illinois, Iowa, and Michigan evaluated for physical and hydraulic properties. NA indicates not available. Cut type was assigned from manufacturer label and visual inspection; for example, “shredded” consisted of mainly thin and long particles while “chipped” mainly consisted of thicker square-shaped particles.

Woodchip Number	Bin	Woodchip Name	Woodchip Source; Manufacturer	"Cut type"	Genus/Species	Softwood or Hardwood mix	Collection Date (MM/DD/YYYY)
1	Municipal Debris	UIUC F&S Mix 1	University of Illinois Facilities and Services Compost Facility	Chipped	NA	Unknown	09/13/2019
2	Municipal Debris	UIUC F&S Mix 2	University of Illinois Facilities and Services Compost Facility	Chipped	NA	Unknown	09/13/2019
3	Municipal Debris	UIUC AgEng Farm Bioreactor Recharge	University of Illinois Agricultural Engineering Farm Bioreactor Recharge	Chipped	NA	Unknown (pine needles observed)	09/30/2019
4	Bagged Mulch	Cedar Chips	Lowes, Champaign, IL	Chipped	suspected *Thuja*	Softwood	10/07/2019
5	Bagged Mulch	Recycled Wood Woodchip Mulch	Menards, Champaign, IL; Wood Ecology Inc.	Shredded and Chipped	NA	Unknown	10/07/2019
6	Bagged Mulch	Cypress Mulch	Prairie Gardens, Champaign, IL; UMS/Ohio Mulch	Shredded and Chipped	suspected *Taxodium*	Softwood	10/07/2019
7	Bagged Mulch	Pine Bark Mulch	Prairie Gardens, Champaign, IL	Bark	*Pinus*	Softwood	10/07/2019
8	Bagged Mulch	Shredded Cedar Mulch	Menards, Champaign, IL	Shredded	suspected *Thuja*	Softwood	10/07/2019
9	Bagged Mulch	Dark Hardwood Mulch	Home Depot, Champaign, IL	Shredded and Chipped	NA	Hardwood	10/07/2019
10	Municipal Debris	Decatur Municipal Woodchips	City of Decatur, IL Forestry Department	Chipped	NA	Unknown	09/10/2020
11	Bulk Supplier/Sawmill	Premium Chipped Hardwood Mulch	Landscape Recycling Center, Urbana, IL	Chipped	NA	Hardwood	09/19/2020

Table 1 (cont.)

Woodchip Number	Bin	Woodchip Name	Woodchip Source; Manufacturer	"Cut type"	Genus/Species	Softwood or Hardwood mix	Collection Date (MM/DD/YYYY)
12	Bulk Supplier/Sawmill	Select Chipped Hardwood Mulch	Landscape Recycling Center, Urbana, IL	Chipped	NA	Hardwood	09/19/2020
13	NRCS Approved	Private Farm Bioreactor Woodchips 1	Xylem LTD, Cordova, IL	Chipped	80% *Acer* (Maple), 20% *Quercus* (Oak)	Hardwood	09/21/2020
14	Bulk Supplier/Sawmill	Hardwood Bioreactor Chips	Xylem LTD, Cordova, IL	Chipped	NA	Hardwood	10/10/2020
15	Bulk Supplier/Sawmill	XylemMat Playground Chips	Xylem LTD, Cordova, IL	Chipped	NA	Hardwood	10/10/2020
16	Bulk Supplier/Sawmill	Davenport Municipal Chipped Mulch	Davenport Compost Center, Davenport, IA	Chipped	*Quercus* (Oak) mix	Hardwood	10/10/2020
17	Municipal Debris	Cedar Rapids Municipal Woodchips	Cedar Rapids Solid Waste Agency, Cedar Rapids, IA	Chipped	NA	NA	10/10/2020
18	Bulk Supplier/Sawmill	Fulton County Bioreactor Woodchips	Corsaw Lumber, Smithfield, IL	Chipped	NA	NA	11/14/2020
19	Bulk Supplier/Sawmill	Large Chips	Chips Groundcover, Holland, MI	Chipped, included bark	*Pinus*	Softwood	11/28/2020
20	Bulk Supplier/Sawmill	Natural Mulch	Chips Groundcover, Holland, MI	Shredded and Chipped	NA	NA	11/28/2020
21	NRCS Approved	Private Farm Bioreactor Woodchips 2	Corsaw Lumber, Smithfield, IL	Chipped	Primarily *Carya* (Hickory) and *Acer* (Maple)	Hardwood	12/01/2020

Woodchips were qualitatively binned to better contextualize the results (Table 1). "Bagged mulch" indicated woodchips were purchased in bags from suppliers; "Bulk supplier/sawmill" chips were sold as bulk products by composting facilities, sawmills, and mulch suppliers; "Municipal debris" was available for free from city or university composting facilities; and "NRCS approved" chips had passed NRCS inspection for use in NRCS-designed bioreactors. Bagged woodchip mulches were studied because they included a variety of sizes and shapes; some bagged woodchips were similar in size to bulk woodchips while some had larger length-to-width ratios. Briefly, Chips #13 and 21 met the USDA-NRCS CPS 605 woodchip specifications and were used in full-size bioreactor installations in Illinois. Chips #8, 9, and 20 were particularly shredded and mulch-like with many fines. Chips #5, 6, and 15 had mainly long, rectangular particles. Chips #3 and 10 contained pieces of pine needles and leaves, respectively, while Chip #17 contained leaves, fines, and small sticks. Chip #7 (bagged "pine bark" from Prairie Gardens, Champaign, IL) was notably large and was excluded from most of the multivariate analyses since it was determined to be an outlier in size and not representative of typical woodchips. Most types contained mainly squared-shaped particles of varying size except for the shredded (Chips #5, 6, 8, 9, and 20) and bark (Chip #7) types, and Chip #10, which was a heterogeneous mixture of chipped particles, longer stick and branch pieces, leaves, and fines (Appendix A).

2.2 PHYSICAL PROPERTY MEASUREMENT

2.2.1 Particle Size by Sieving

The particle size distribution analysis followed standard methods (ANSI/ASABE, 1992), and in short, 70 to 300 g air-dried woodchips (enough to fill the top pan) were shaken for five minutes using a series of seven mesh sizes (W.S. Tyler RX-812 Coarse Sieve Shaker, Mentor,

OH, USA; mesh sizes: 3.2, 6.3, 12.5, 19.0, 25.0, 37.5 mm and either 1.7 or 50 mm). The largest woodchip (Chip #7, Table 1) required mesh sizes of 6.3, 19, 25, 38, 50, 75, and 100 mm. Particle size parameters of D_{10}, D_{50}, D_{60}, D_{90} were estimated using linear interpolation and uniformity coefficient (UC) was calculated as the D_{60} divided by the D_{10}. D_x is the size at which x% of woodchip particles are smaller by mass (e.g., woodchip media with a D_{10} of 7.0 mm would have 10% of the woodchips by mass smaller than 7.0 mm).

Moisture content was determined on a subset of woodchips every day particle size analysis was performed by drying 20 to 60 g woodchip at 70 °C until reaching a constant weight (Thermo Fisher Scientific, 180L Gravity Oven, Model Number 51030521, Pittsburg, PA, USA; performed in triplicate). This consistent dry weight was defined as less than 1% change in mass from the prior measurement whereas measurements were generally 24 h apart over the 3-4 d required. Moisture content as a percent was calculated using Equation 1:

$$mc = \frac{(M_w - M_d)}{M_w} * 100 \quad (1)$$

where mc is the moisture content on a wet basis (%), M_w is the wet mass of woodchips (g), and M_d is the final oven-dried mass of woodchips (g).

2.2.2 Particle Size by Manual Measurement

Woodchip particle size was also measured by hand using a digital caliper (Tool Shop 6" Stainless Steel Digital Caliper, Model Number MEN-0007_48MC) on a random subsample of 30 air-dried woodchips of each type (Figure 2). A sample size of 30 is generally sufficient to approximate a normal distribution (Hogg et al., 2015). The random sampling was accomplished by grabbing a handful of well-mixed woodchips from the storage tub and then selecting individual woodchips from that subsample without looking. The woodchips were envisioned as

rectangular prisms, with measurement of the length (long axis), width (medium axis), and depth (short axis) of each particle. Regardless of attempts to minimize bias (e.g., one person performed all the measurements), these manual measurements necessarily excluded fines and particles smaller than 3 mm due to human hand constraints. While this constraint could have caused a larger difference between manual and sieve measurements for woodchip types with smaller D_{10} values, most of the small particles excluded in the manual measurements had a small mass and likely didn't strongly impact the mass-based sieve parameters.

Figure 2. Manual measurement of woodchip width using a digital caliper.

2.2.3 Jar Porosity and Bulk Density

Total and drainable porosity and bulk density were measured in triplicate by packing three to five layers of air-dried woodchips into 1-L beakers, filling with water, and saturating for 24 h (Ima and Mann, 2007). Each layer was approximately 3 cm thick and packed by gently tapping the beaker on the lab bench and tamping with a fisted hand, five times each. Porosity was calculated with Equation 2:

$$n = \frac{\frac{M_{water}}{\rho_{water}}}{V_T} \times 100 \quad (2)$$

Where n is the porosity (%), M_{water} is the water mass in the woodchip-filled beaker (g), ρ_{water} is the density of water (g mL^{-1}), and V_T is the total beaker volume (mL). Drainable porosity was measured immediately after filling the woodchip-filled beaker with water, while total porosity was measured after 24 h of saturation after topping up the woodchip-filled beaker. Moisture content was measured coinciding with each porosity test (Section 2.2.1) which allowed dry bulk density and particle density to be calculated based on the jar measurements (Equations 3 and 4):

$$\rho_{bd} = \frac{\frac{M_{db}}{V_b}}{1000} \quad (3)$$

$$\rho_{particle} = \frac{\rho_{bd}}{1-\frac{n_T}{100}} \quad (4)$$

where ρ_{bd} is the oven-dried bulk density of woodchips (kg m^{-3}), M_{db} is the oven-dried mass of woodchips in the beaker (g), and V_b is the volume of the beaker (m^3), $\rho_{particle}$ is particle density (kg m^{-3}), and n_T is the total porosity (%). Because beaker volume is an important parameter for these calculations, the volumes of the beakers were determined (n = 5 times per beaker) by measuring the mass of a beaker filled with water to a preset fill line, subtracting the mass of the empty beaker, and dividing by the density of water at standard conditions (998.2 kg m^{-3}).

2.2.4 Nutrient Content

Woodchip carbon, nitrogen, and phosphorus contents were determined by an external laboratory (triplicate samples; combustion analysis and digestion method, Brookside Laboratories Inc., New Bremen, OH, USA).

2.3 SATURATED HYDRAULIC CONDUCTIVITY MEASUREMENTS

2.3.1 Permeameter Set-up

Three PVC permeameter columns (20 cm diameter; either 67 or 77 cm length) were constructed in the Christianson I-DROP Laboratory at the University of Illinois at Urbana-Champaign following standard methods (ASTM, 2019) (Figure 3). The permeameters were connected to the constant head tank with vinyl tubing and PVC fittings (2.5 cm diameter) and the outlet pipe (5.0 cm diameter) was attached approximately 4 cm from the top of the permeameter (Figure 4). Perforated plates were created by drilling staggered 0.48 cm diameter holes in plastic dinner plates to create approximately 40% open area. Springs were mounted inside the permeameter to the hold the perforated plates in place (Figure 5).

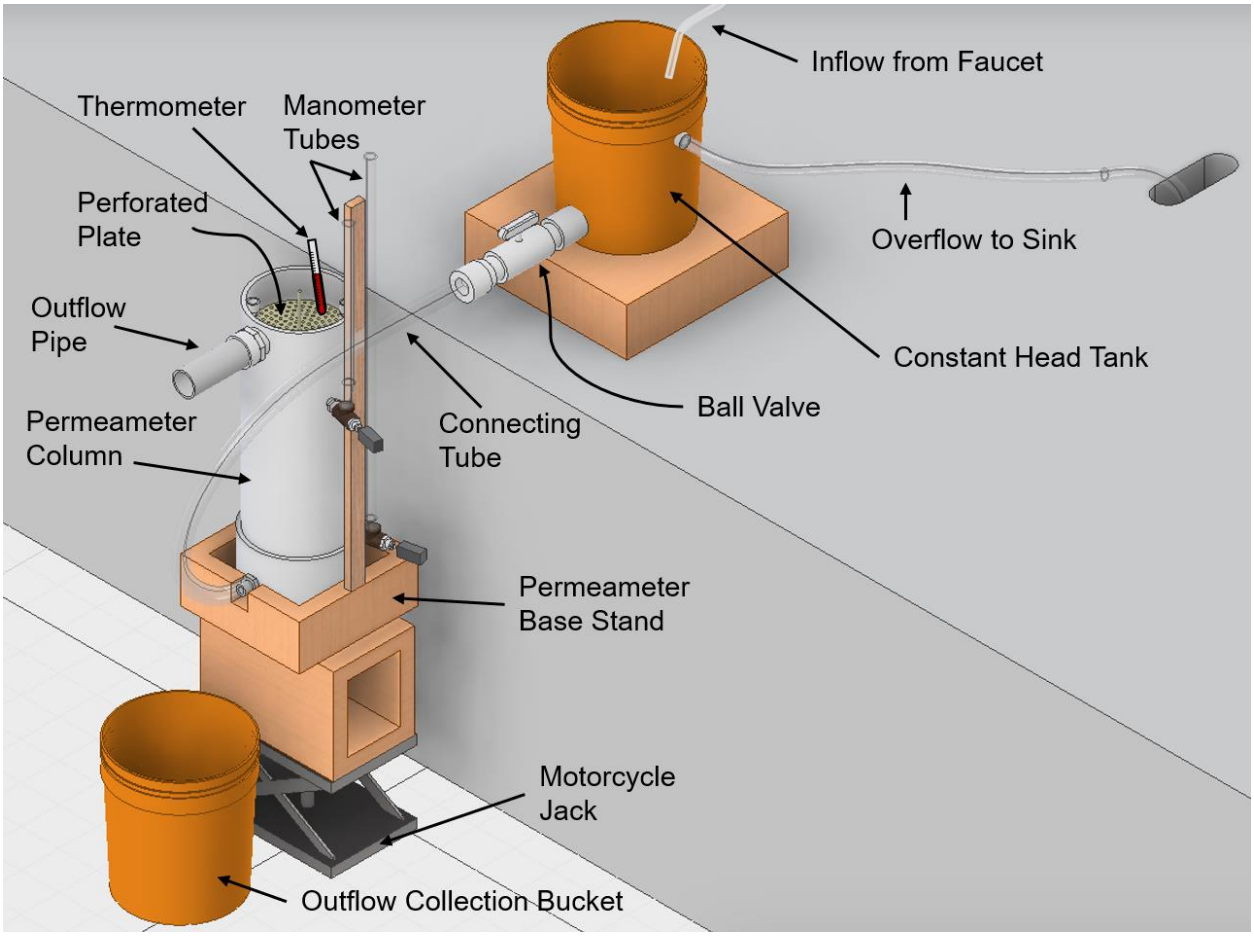

Figure 3. Permeameter set-up in the Christianson I-DROP laboratory at the University of Illinois for estimating woodchip saturated hydraulic conductivity.

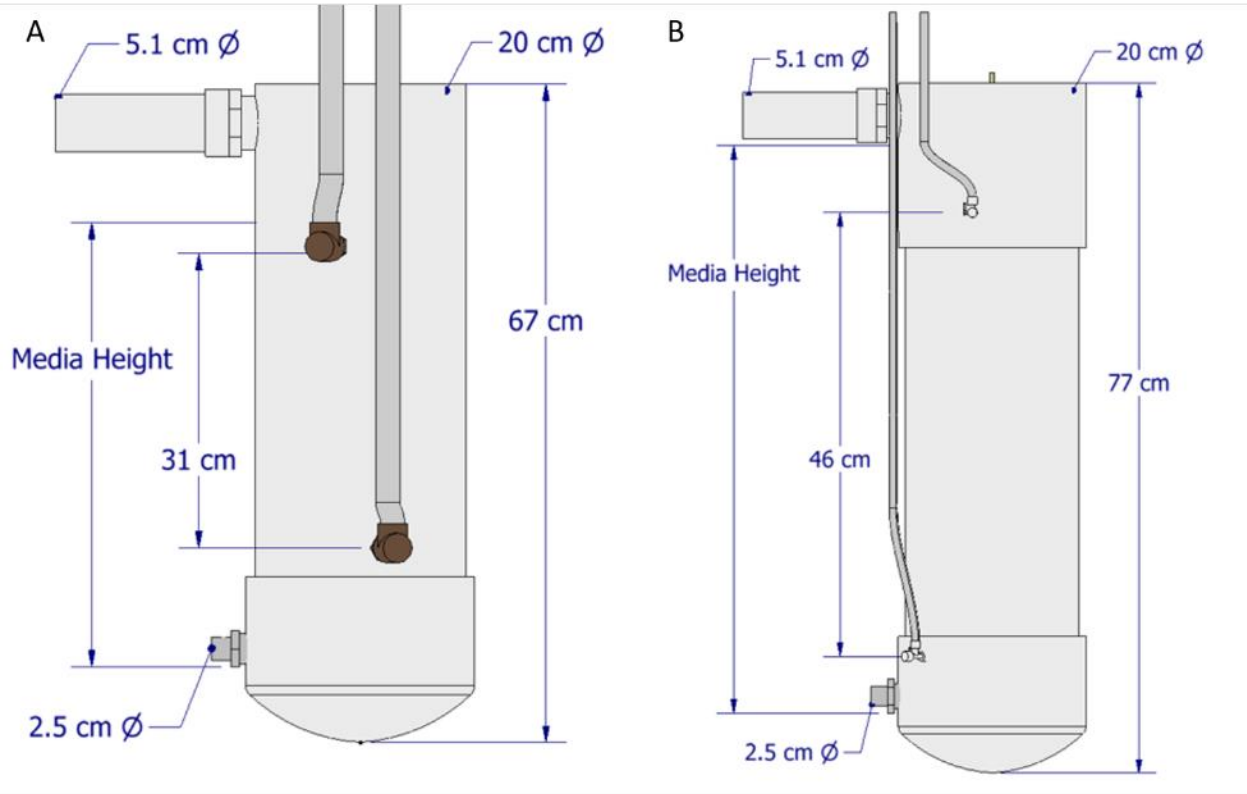

Figure 4. Side view diagram with dimensions of 67 cm height, 31 cm flow length (A) and 77 cm height, 46 cm flow length (B) permeameters. Media height varied slightly with each replicate. Manometer measuring board not shown.

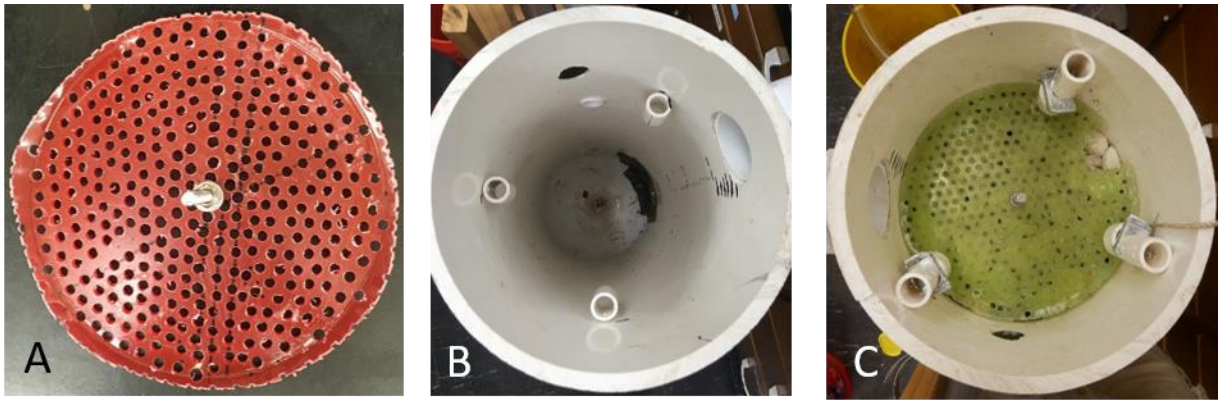

Figure 5. Perforated plate (A), permeameter column with three mounts for springs (B), and perforated plate on top of permeameter column filled with gravel (C).

Per standard guidelines, manometer outlets were installed 31 cm apart on the sides of two permeameter columns and 46 cm apart on the third permeameter column (Figure 4). The longer manometer length was built on the third permeameter to enable easier measurements at lower

hydraulic gradients. However, both permeameter flow lengths exceeded the minimum requirements (flow length ≥ permeameter diameter) and enabled measurement of flow at multiple hydraulic gradients lower than 0.06. Clear plastic tubing, 1.3 cm diameter for the 31 cm length permeameters and 0.6 cm diameter for the 46 cm length permeameter, was attached to the outlets and mounted vertically on a measuring board graduated at 0.2 cm intervals. A constant head tank was created from a 19-L plastic bucket by installing a 3.8 cm ball valve at the base and installing a 1.3 cm diameter overflow outlet 2.5 cm from the bucket top. The water for the constant head tank was provided by the laboratory sink faucet (Figure 3).

2.3.2 Saturated Hydraulic Conductivity Testing and Calculation

Testing was done in triplicate on twenty-one woodchip types based on standard methods for soils (ASTM, 2012, 2019). For high compaction tests, woodchips were packed in three to five equal layers and tamped 25 times per layer using a 2.5 kg manual soil hammer with a 31 cm drop height. The layers were generally 0.7 to 1.4 kg (air-dried weight) and 9 to 15 cm (three to five layers) or 12 to 20 cm (three to five layers layers) thick for woodchip media heights of approximately 45 and 60 cm in the 67 and 77 cm length permeameters, respectively. The woodchips were slowly saturated from the bottom and were left saturated for at least 24 hours prior to commencing the K_{sat} test. Subsamples of the woodchips used to pack the permeameter were collected for moisture content analysis following the procedures in Section 2.2. Outflow from the permeameter was measured at 10 increments of hydraulic head loss, ten times each, using 500-, 1000-, and 2000-mL graduated cylinders or 19-L buckets and a stopwatch. The bucket was used for higher flowrates required for the gravel and the reduced compaction tests and volume was estimated based on the tared weight of water collected (OHAUS Catapult 1000

Scale, Model Number C11P75, Parsippany, NJ, USA). The hydraulic head difference was adjusted by partially opening and closing the valve and by lifting the permeameter up and down using the motorcycle jacks. Per standard guidelines, flow measurements were not recorded until the head difference was stable which was usually achieved within ten minutes.

Saturated hydraulic conductivity was calculated using Darcy's Law (Equations 5 and 6) which states that flow through a porous medium is proportional to the hydraulic gradient, sample area, and a constant:

$$Q = K_{sat} \frac{\Delta H}{L} A \tag{5}$$

$$q = K_{sat} i \tag{6}$$

where Q is the flowrate ($cm^3\ s^{-1}$), K_{sat} is the saturated hydraulic conductivity ($cm\ s^{-1}$), ΔH is the pressure head loss through the sample (cm), L is the length of the sample (cm), A is the cross-sectional area of the sample (cm^2), q is the specific discharge ($cm\ s^{-1}$), and i is the hydraulic gradient ($cm\ cm^{-1}$).

The specific discharge (q) and hydraulic gradient (i) data (Appendix A) were non-linear as has been previously reported by (Feyereisen and Christianson, 2015; Ghane et al., 2014; Ghane et al., 2016). Thus, linear regressions were performed on natural logs of q and i and K_{sat} was determined by exponentiating the regression line slope (Equation 7). Hydraulic gradients ranging from 0.004 to 0.06 were used based on a realistic range for field bioreactors (e.g., limited to gradients less than a ΔH of 0.9 m over a 15 m long bioreactor = 0.06). Viscosity adjustments, based on the temperature of the water measured in the permeameter, were applied to the K_{sat} measurements following standard procedures (ASTM, 2019). Reported K_{sat}s are averages of all three replicates.

2.3.3 Permeameter validation with gravel

Woodchip size characteristics and K_{sat}s, as well as the methods used to determine these parameters, have ranged widely across literature (e.g., Burbery et al., 2014; Christianson et al., 2010; Feyereisen and Christianson, 2015; Ghane et al., 2014; Robertson and Merkley, 2009; Subroy et al., 2014; van Driel et al., 2006). Three sizes of gravel (Table 2) were used to validate the permeameter set-up and K_{sat} estimation method with the assumption that properties for commercially available gravel sources would be more consistent (and more consistently reported) than woodchips. The same procedures as described in section 2.4.2 were followed except the gravel replicates were not tamped.

Table 2: Three types of gravel tested for saturated hydraulic conductivity to calibrate the permeameter system.

Gravel Number	Gravel Name	Source	Qualitative size descriptor
G1	Vigoro Marble Chips	Home Depot, Champaign, IL	Large
G2	MSI River Rock	Home Depot, Champaign, IL	Medium
G3	Vigoro River Pebbles	Home Depot, Champaign, IL	Small

2.3.4 Woodchip Compaction Experiments

Effects of woodchip compaction (e.g., possible compaction caused by other woodchips or soil overburden in a field bioreactor) on bulk density and saturated hydraulic conductivity were investigated by adjusting the permeameter tamping procedure. Saturated hydraulic conductivity was measured on four woodchip types (#5, 13, 15, and 21) by packing them at the lowest density possible (0 tamps per layer) and at a medium packing density (10 tamps per layer) in addition to the high compaction described above (25 tamps per layer). Chip #5 consisted of long and narrow particles; Chip #13 was medium-length square particles meeting NRCS CPS 605; Chip #15 was

shorter, narrow, “mulchy” particles; and Chip #21 was large square-shaped particles meeting NRCS CPS 605 (Figure 1, Appendix A). To create a more complete understanding of woodchip and soil overburden compaction, bulk density (but not K_{sat}) of Chips #4, 14, 18, 20, and 21 was additionally measured in the permeameter column using 0, 10, 25, and 50 tamps per layer.

2.3.5 Permeameter Column Bulk Density and Porosity Measurement

Bulk density and drainable porosity were estimated using the jar tests mentioned above (Section 2.2.3) and were also estimated using the permeameter. Bulk density of the woodchips and gravel in the permeameter columns was calculated from the total material mass, weighed by layer (OHAUS Catapult 1000 Scale, Model Number C11P75, Parsippany, NJ, USA), and permeameter volume filled by the woodchips (Equation 8).

$$\rho_p = \frac{M_{wc}}{\left(\pi\left(\frac{d^2}{4}\right)h_{wc}\right)+\left(\frac{2}{3}\pi\left(\frac{d^3}{8}\right)\right)} \quad (8)$$

Where ρ_p is the permeameter packing density, M_{wc} is the total material mass in the column (kg), d is the inner diameter of the permeameter (m^3), and h_{wc} is the height of the woodchips in the permeameter (m).

Drainable porosity in the permeameters was measured from the mass of water (OHAUS Catapult 1000 Scale, Model Number C11P75, Parsippany, NJ, USA) drained from the columns into empty buckets after 24 h (Equation 9).

$$n = \frac{M_{dw}\rho_w}{\left(\pi\left(\frac{d^2}{4}\right)h_{dwc}\right)} \times 100 \quad (9)$$

Where n is the porosity (%), M_{dw} is the mass of drained water (kg), ρ_w is the density of water (kg m^{-3}), d is the inner diameter of the permeameter (m^3), and h_{dwc} is the height of the drained

woodchips (m) (i.e., the height of the woodchips above the bottom edge of the drain port). Total porosity was not measured in the permeameters because the drainable porosity or effective porosity is used for bioreactor design (Illinois NRCS, 2021).

2.3.6 “Chipometer” Permeameter Measurements

Saturated hydraulic conductivity was measured on Chips #1-6 on an alternate permeameter system called the “Chipometer” (Figure 6) designed to be an inexpensive and transportable tool for field-site assessments of potential bioreactor woodchip media. The Chipometer had similar dimensions to the constant head permeameters constructed in the Christianson I-DROP Lab (20 cm diameter, 30 cm length between manometer ports) but had downward flow with constant water level provided by a hose directly attached to the permeameter. Only one replicate was tested and these data were not limited to hydraulic gradients lower than 0.06 because it difficult to use this system at lower gradients.

Figure 6. “Chipometer” Permeameter constructed in the ABE Hydraulics Lab at the University of Illinois.

2.4 DATA ANALYSIS

Relationships between woodchip properties were assessed with simple and multiple linear regressions. Stepwise multiple linear regression models of K_{sat} based on 19 properties (permeameter drainable porosity and bulk density; jar drainable porosity, total porosity, and bulk density; particle density; D_{10}; D_{50}; D_{60}; D_{90}; UC; and average and median length, width, depth, and length-to-width ratio) were calculated using the "ols_step_both_p" function from the "olsrr" package in R (Hebbali, 2020; R Core Team, 2020). Homoscedasticity and residual normality for the multiple linear regression models were assessed with residual versus fitted value plots and residual quantile-quantile plots, respectively. Means of bulk density and porosity from the jar and permeameter methods were compared with paired t-tests. Mean values for K_{sat}, length, width, depth, and length-to-width ratio of each woodchip type were compared with Tukey's honestly significant different test using the "HSD.test" function in the "agricolae" package in R (de Mendiburu, 2020).

CHAPTER 3: RESULTS AND DISCUSSION

3.1 SATURATED HYDRAULIC CONDUCTIVITY

3.1.1 High Compaction Regime

The K_{sat} of 20 types of woodchips commonly available in the United States Midwest region tested with high compaction ranged from 0.10 to 2.05 cm s^{-1} (mean ± standard deviation: 1.04 ± 0.60 cm s^{-1}; median: 0.99 cm s^{-1}; Table 3) and were most correlated with drainable porosity (permeameter-method) and the D_{50} median diameter when evaluated as discrete parameters (Figure 7; R^2 = 0.31 and 0.25, respectively). Chip #7, the bagged large Pine Bark, was substantially larger than typical woodchips used for bioreactors (median size, D_{50} = 61 mm; K_{sat} 4.48 cm s^{-1}; Table 3; not shown in Figure 7), thus was excluded from further analyses. The high compaction procedure of 25 tamps per layer developed from the ASTM standard provided near maximum compaction (see section 3.3) but allowed the most consistent comparison across all woodchips. Under this compaction, the values were relatively low compared to most other woodchip K_{sat} studies that have generally documented values of at least approximately 3 cm s^{-1} for woodchips on the order of 8 - 13 mm (Chun et al., 2009; Christianson et al., 2010; Feyereisen and Christianson 2015; and Ghane et al. 2014). However, there is a range in reported K_{sat} values with *in-situ* values ranging from 0.47 to 10 cm s^{-1} for coarse woodchips (Robertson and Merkley, 2009) and lower values of 0.12 and 1.2 cm s^{-1} reported for fine sawdust and coarse woodchips, respectively, by van Driel et al. (2006).

Table 3. Saturated hydraulic conductivity (under high compaction), dry bulk density, porosity, and particle density of all 21 woodchip types. A * indicates values are from one replicate only because moisture content was not recorded in some initial permeameter runs.

#	Woodchip Description	Woodchip Bin	K_{sat} cm s^{-1}	Bulk Density - Permeameter kg m^{-3}	Drainable Porosity - Permeameter %	Bulk Density - Jar kg m^{-3}	Drainable Porosity - Jar %	Total Porosity - Jar %	Particle Density kg m^{-3}
1	Composting Facility Mixed Chips	Municipal Debris	0.75 ± 0.48	282*	38 ± 5	251 ± 7	62 ± 1	73 ± 0	1027 ± 18
2	Composting Facility Mixed Chips	Municipal Debris	0.92 ± 0.75	326 ± 21	34 ± 1	287 ± 8	60 ± 1	66 ± 1	923 ± 22
3	Mixed Chips	Municipal Debris	1.96 ± 1.35	236*	35 ± 1	214 ± 4	61 ± 2	70 ± 2	772 ± 46
4	Bagged Cedar Mulch	Bagged Mulch	1.99 ± 0.81	160*	42 ± 0	142 ± 8	61 ± 1	73 ± 1	550 ± 4
5	Bagged Woodchip Much	Bagged Mulch	0.51 ± 0.35	219*	40 ± 3	199 ± 2	65 ± 1	73 ± 1	789 ± 35
6	Bagged Cypress Mulch	Bagged Mulch	1.19 ± 0.58	174 ± 14	47 ± 2	137 ± 1	77 ± 1	83 ± 1	865 ± 54
7	Bagged Pine Bark Mulch	Bagged Mulch	4.48 ± 1.05	207 ± 1	47 ± 2	165 ± 16	67 ± 4	70 ± 4	600 ± 25
8	Bagged Shredded Cedar Mulch	Bagged Mulch	0.10 ± 0.04	166 ± 9	34 ± 4	155 ± 9	61 ± 1	67 ± 1	662 ± 33
9	Bagged Hardwood Mulch	Bagged Mulch	0.20 ± 0.08	294 ± 13	34 ± 3	192 ± 13	74 ± 2	79 ± 1	1002 ± 50
10	Municipal Tree Debris Mixed Chips	Municipal Debris	1.19 ± 0.27	224 ± 7	40 ± 1	175 ± 12	66 ± 1	69 ± 2	725 ± 57
11	Composting Facility Mixed Hardwood Chips	Bulk Supplier/Sawmill	0.40 ± 0.15	262 ± 8	36 ± 2	209 ± 12	63 ± 2	74 ± 1	894 ± 43
12	Composting Facility Mixed Hardwood Chips	Bulk Supplier/Sawmill	0.47 ± 0.18	227 ± 29	39 ± 2	199 ± 9	65 ± 1	75 ± 1	884 ± 23
13	Maple-Oak Mixed Chips (NRCS spec)	NRCS Approved	1.24 ± 0.42	265 ± 6	40 ± 2	232 ± 8	62 ± 1	73 ± 1	971 ± 48
14	Mixed Hardwood Chips	Bulk Supplier/Sawmill	0.54 ± 0.20	243 ± 16	41 ± 7	209 ± 2	61 ± 2	74 ± 2	862 ± 52
15	Bagged Hardwood Playground Chips	Bulk Supplier/Sawmill	0.66 ± 0.49	233 ± 7	37 ± 2	211 ± 5	64 ± 1	72 ± 1	789 ± 10
16	Municipal Mixed Oak Chips	Bulk Supplier/Sawmill	1.77 ± 1.40	265 ± 10	39 ± 4	239 ± 1	64 ± 0	73 ± 1	983 ± 27

Table 3 (cont.)

#	Woodchip Description	Woodchip Bin	K_{sat} cm s^{-1}	Bulk Density - Permeameter kg m^{-3}	Drainable Porosity - Permeameter %	Bulk Density - Jar kg m^{-3}	Drainable Porosity - Jar %	Total Porosity - Jar %	Particle Density kg m^{-3}
17	Municipal Tree Debris Mixed Chips (Derecho)	Municipal Debris	1.06 ± 0.98	289 ± 12	40 ± 1	255 ± 5	65 ± 1	73 ± 2	1017 ± 69
18	Mixed Hardwood Chips	Bulk Supplier/Sawmill	1.64 ± 0.58	255 ± 15	42 ± 2	211 ± 16	67 ± 1	76 ± 0	960 ± 76
19	Mixed Softwood Chips	Bulk Supplier/Sawmill	1.26 ± 0.48	210 ± 10	42 ± 1	181 ± 5	72 ± 1	79 ± 1	911 ± 20
20	Mixed Shredded Mulch	Bulk Supplier/Sawmill	2.05 ± 1.47	199 ± 7	50 ± 2	157 ± 17	77 ± 3	83 ± 2	982 ± 43
21	Mixed Hardwood Chips (NRCS spec)	NRCS Approved	0.87 ± 0.69	321 ± 15	37 ± 2	266 ± 9	60 ± 1	71 ± 1	997 ± 13

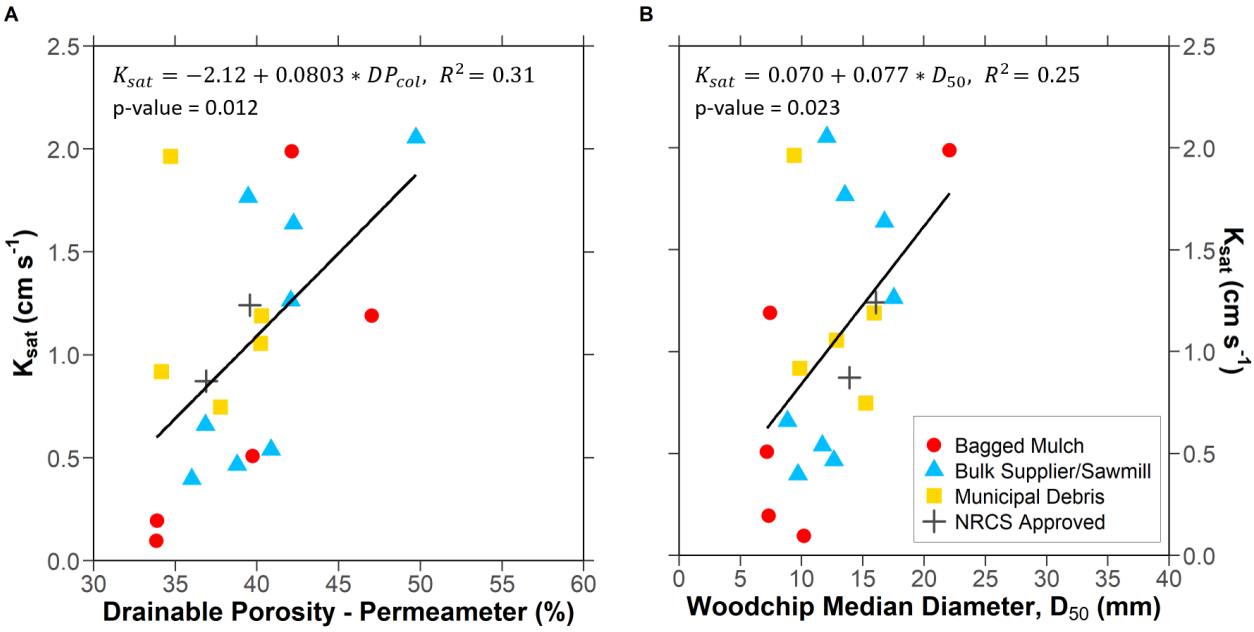

Figure 7. Saturated hydraulic conductivity versus drainable porosity determined using the permeameter method (A) and versus the woodchip median diameter, D_{50}, (B) of twenty woodchip types sourced in Illinois, Iowa, and Michigan and tested under high compaction (25 tamps per layer).

Permeameter drainable porosity and woodchip median width were the only significant predictor variables for K_{sat} in the stepwise multiple linear regression analysis which evaluated 19 parameters in a bidirectional process (i.e. variables were entered or removed from the model in succession based on significance level). The resulting model was (Equation 10):

$$K_{sat} = -2.72 + 0.081\, DP_{perm} + 0.048 W_{med} \quad (10)$$

where DP_{perm} is the permeameter drainable porosity (%), W_{med} is the median width, and the corresponding model coefficient of determination and p value were $R^2 = 0.48$ and $p = 0.0038$. This two variable model improved the fit by 1.5 times compared to the discrete regression using only permeameter drainable porosity (R^2 of 0.48 vs. 0.31, respectively). While the multiple linear regression model did improve the regression goodness-of-fit compared to any individual parameter, it only improved upon the single-variable prediction of permeameter drainable

porosity by 0.17. In other words, it only explained 17% more variability than the best single-variable prediction, and still explained less than half of the total variability of these woodchip data.

Both the individual and multiple regressions included constant terms for the best fit, however these are not be physically possible (e.g. -2.12 cm s^{-1} K_{sat} at a 0% drainable porosity, Figure 7B). Despite these limitations, the models should still be applicable to the range of values used to develop them. Specifically, because the woodchips were highly compacted, these drainable porosities are likely the minimum that would be measured, thus these models would not be used for situations with 0 drainable porosity.

It was hypothesized that parameters such as D_{10}, UC, length-to-width ratio, and bulk density would also be correlated with K_{sat} in the multiple linear regression model, but these were not significant. However, the multiple regression model was notable when compared to the discrete parameter regressions because woodchip median width, not the sieve analysis-derived D_{50} (e.g., Figure 7B), was the second most significant K_{sat} predictor once the model included permeameter drainable porosity. While D_{50} did not appear in the multiple linear regression, median width and D_{50} were positively correlated (R^2 = 0.47, p-value < 0.001, Section 3.3).

The strength of the explanatory relationships may have been limited by the relatively small range of K_{sat} values, which was likely related to the high packing densities (160-326 kg m^{-3}; Table 3; Section 3.3). Additionally, the number of observations (n=20) was small compared to the number of predictor variables (19). Hair et al. (2009) suggests there should be least five observations for every independent variable in multiple regression analysis, however all 19 of these variables were not independent.

The small range of K_{sat} values and lack of consistent trends in K_{sat} across the qualitatively-described woodchip bins (e.g., NRCS Approved) indicated that at relatively maximum compaction, there was little variability across woodchip types K_{sat} values (< 2.0 cm s^{-1}). Specifically, the NRCS-approved woodchips had values close to the median of 1.0 cm s^{-1} (1.24 and 0.87 cm s^{-1} for Chips #13 and 21, respectively), while the rest of the bins had ranges similar to the full range of all chip types. The Bulk Supplier/Sawmill woodchips exhibited some of the highest and some of the lowest values for K_{sat} (2.05 and 1.77 cm s^{-1} for Chips #20 and 16, respectively, compared to 0.40 and 0.47 cm s^{-1} for Chips #11 and 12, respectively). The Bagged Mulches resulted in the two lowest values for K_{sat} among all types for two shredded-type chips (0.20 and 0.10 cm s^{-1} for Chips #9 and 8, respectively), but also included one of the highest K_{sat} values (1.99 cm s^{-1} for Chip #4). Most of the Municipal Debris woodchips had K_{sat} values near or exceeding the median of 1.0 cm s^{-1}, further suggesting that at maximum compaction, free woodchips from local tree trimmings have similar flow properties to "better" woodchips. However, recommendations for woodchip suitability for bioreactors cannot be made from these results alone as the high compaction regime may not accurately represent in field conditions. Thus, these results must be contextualized with the reduced packing regime and bulk density results (Sections 3.1.2 and 3.3).

3.1.2 Reduced Packing Regime

Using reduced packing regimes (0 and 10 tamps per layer), the K_{sat} of Chips #5, 13, and 21 notably increased compared to the high compaction regime (Figure 8B). For example, the K_{sat} of Chip #5 was nearly 12 times greater when it was not compacted compared to the high compaction (6.1 vs. 0.51 cm s^{-1} for 0 and 25 tamps, respectively), and the NRCS-approved

woodchips were approximately 6 and 7 times greater (7.4 vs. 1.24 and 5.87 vs 0.87 cm s^{-1}, respectively, for Chips #13 and 21). These higher values align more closely with values reported by Christianson et al. (2010) and Feyereisen and Christianson (2015) of 4.5 to 9.5 cm s^{-1} at 220-300 kg m^{-3} reported bulk densities for woodchips in the 10-13 mm size range.

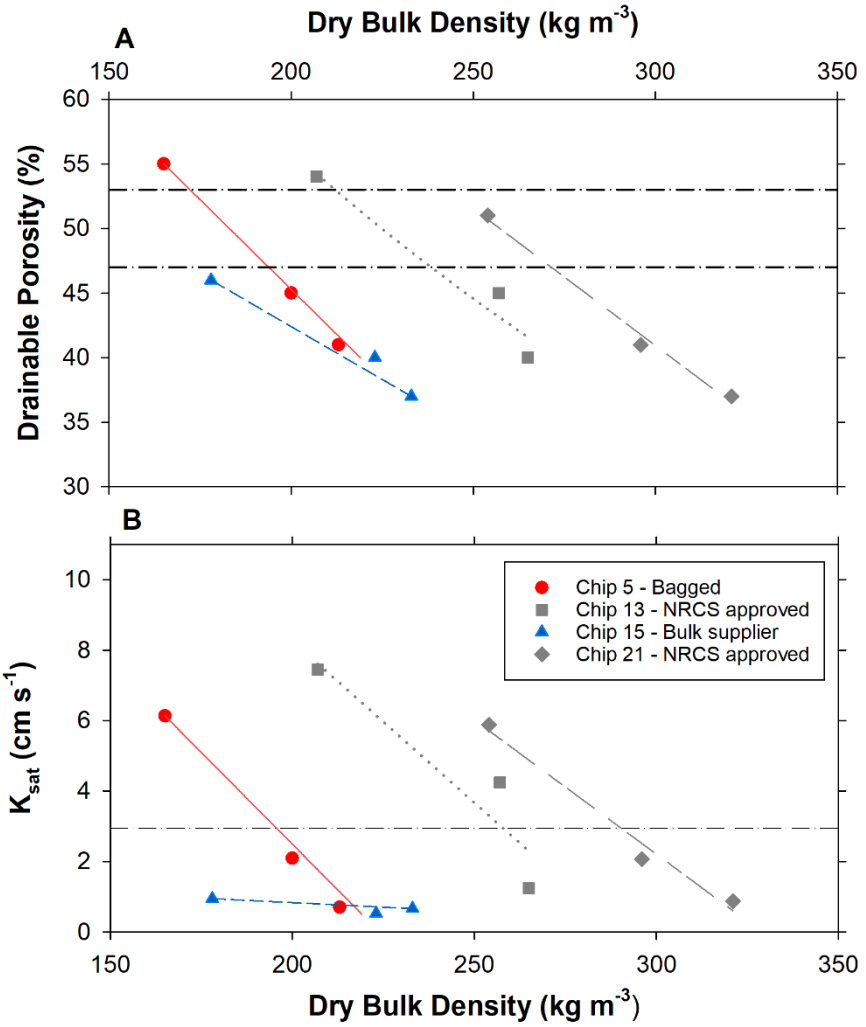

Figure 8. Scatterplots of permeameter drainable porosity (A) and saturated hydraulic conductivity (B) versus permeameter bulk density for four chip types tested under reduced compaction. For each type, the lowest, intermediate, and highest bulk densities were from 0, 10 and 25 (standard) tamps per layer, respectively. Reference lines indicate NRCS default design values.

In contrast to Chips #5, 13, and 21, the K_{sat} of Chip #15 only increased by a factor of 1.4 under the low compaction regime compared to the high compaction treatment and had a slightly

lower K_{sat} under medium compaction than under high compaction (0.94 and 0.52 vs. 0.66 cm s^{-1}, respectively; Table 4; Figure 8B). However, there was similar high variability in the mean Ksat values under all three compaction methods (standard deviations at low, medium, and high compaction: 0.25, 0.48, and 0.49 cm s^{-1}, respectively) indicating the differences between methods may not be significant. The different performance of Chip #15 compared to the other three woodchip types may be explained by the shorter and more square nature of Chip #15 compared to the long and skinny nature of Chip #5, and larger median diameters of Chips #13 and 21. The shorter nature of the Chip #15 particles likely contributed to a denser, less porous packing arrangement (Table 4), leading to a smaller increase in K_{sat} under the reduced compaction regime. In other words, the more shredded, mulchy nature of Chip #5 may have prevented tight settling of the woodchip particles and resulted in higher porosity and permeability than the similarly sized (in terms of D_{50}) Chip #15.

Table 4. Saturated hydraulic conductivity, bulk density and drainable porosity of woodchips tested with reduced compaction regimes.

#	Woodchip Description	Woodchip Bin	Tamps per layer	K_{sat} cm s^{-1}	Bulk Density - Permeameter kg m^{-3}	Drainable Porosity - Permeameter %
5	Bagged Woodchip Much	Bagged Mulch	0	6.13 ± 5.33	165 ± 4.6	55 ± 1.8
5	Bagged Woodchip Much	Bagged Mulch	10	2.09 ± 0.98	200 ± 6.1	45 ± 2.9
13	Maple-Oak Mixed Chips (NRCS spec)	NRCS Approved	0	7.44 ± 2.53	207 ± 2.3	54 ± 2.2
13	Maple-Oak Mixed Chips (NRCS spec)	NRCS Approved	10	4.24 ± 4.37	257 ± 10.3	45 ± 4.0
15	Bagged Hardwood Playground Chips	Bulk Supplier/Sawmill	0	0.94 ± 0.25	178 ± 1.1	46 ± 2.4
15	Bagged Hardwood Playground Chips	Bulk Supplier/Sawmill	10	0.52 ± 0.48	223 ± 8.6	40 ± 0.7
21	Mixed Hardwood Chips (NRCS spec)	NRCS Approved	0	5.87 ± 3.01	254 ± 5.5	51 ± 0.7
21	Mixed Hardwood Chips (NRCS spec)	NRCS Approved	10	2.07 ± 1.84	296 ± 15.2	41 ± 4.7

The relatively narrow range of K_{sat} values across twenty woodchips sourced from three Midwestern states indicated that when woodchips are tightly compacted the K_{sat} tends to be on the order of 0.5 to 2.0 cm s^{-1}. However, the relatively low predictive power of both the discrete and multiple parameter regression models illustrated the insensitivity of K_{sat} to woodchip physical parameters when highly compacted. Testing a selected set of woodchips under a range of compactions (Figure 8B) illustrated woodchip K_{sat} is much more sensitive to compaction than to woodchip type. The K_{sat} values under reduced compaction may be more representative of *in situ* values. However, there is a notable lack of *in situ* bioreactor bulk densities reported (Section 3.3) to relate to these laboratory results.

3.1.3 Chipometer Permeameter

Saturated hydraulic conductivity values for Chips #1-6 measured with the Chipometer permeameter were relatively similar with all ranging from 0.42 to 0.65 cm s^{1} except for Chip #4 which had a value of 1.23 cm s^{-1}. These results were not strongly correlated with the K_{sat} values measured with the I-DROP permeameters (Figure 9, $R^2 = 0.32$). This may been due to the lack of replicates and higher gradient data used for the Chipometer measurements as well as the high compaction limiting the overall range of K_{sat} values.

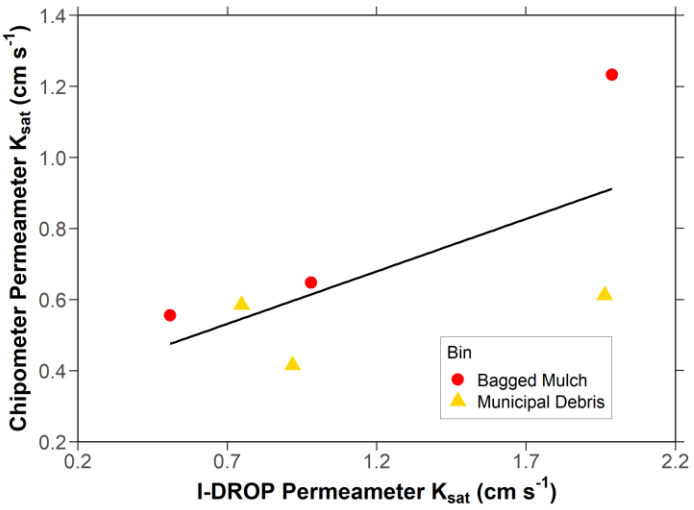

Figure 9. Scatterplot of saturated hydraulic conductivity measured with the I-DROP permeameter system and the Chipometer permeameter.

3.1.4 Gravel

Gravel tested in the permeameters was a successful calibration procedure, although findings and additional literature review suggested that gravel K_{sat} values, like woodchips, vary even for a given qualitative size. Saturated hydraulic conductivity and drainable porosity of the gravel ranged from 1.3 to 13.9 cm s^{-1} and 24 to 48%, respectively, at median sizes ranging from 9.9 to 23.3 mm. Gupta (2017) reported that "coarse gravel" ranged in K_{sat} from 1.2 to 10.0 cm s^{-1} but did not report the specific size. The coarsest gravel tested here had a K_{sat} of 13.9 cm s^{-1}, which was higher than the previously reported range, but this testing had large variability (e.g., standard deviation of 10 cm s^{-1}; Table 5). Judge (2013) reported larger K_{sat} values of 20 and 15 cm s^{-1} for "gravel" and "fine gravel" with median sizes of 8 and 5 mm, respectively. Those sizes were most similar to the "small" gravel tested here (D_{50} = 9.9 mm) which had a much lower Ksat of 1.3 ± 0.3 cm s^{-1} compared to the past finding. However, this is likely due to the presence of sand in this "small" gravel, reflected by the smaller D_{10} than the "medium" and "large" gravel, as Gupta (2017) reported the K_{sat} of "coarse" and "medium" sand ranges 1.2×10^{-4} to 0.58 cm s^{-1}.

The values here seemed more aligned with Bordier and Zimmer (2000) who reported K_{sat} values of 14.5 and 17.6 cm s^{-1} for gravel ranging in size from 10-14 mm and 20-40 mm, respectively. Fetter (2001) suggested that porosities of "well-sorted gravel" usually range from 25 to 50% which was nearly identical to that determined here.

Table 5. Gravel saturated hydraulic conductivity, bulk density, porosity, and size parameters. BD – Perm and DP – Perm: bulk density and drainable porosity by permeameter method, respectively. DP – Jar, TP – Jar, BD – Jar, PD – Jar: drainable and total porosity, and bulk and particle density by jar method, respectively.

#	Qualitative Size Descriptor	K_{sat}	BD - Perm	DP - Perm	DP - Jar	TP - Jar	BD - Jar	PD - Jar	D_{10}	D_{50}	D_{90}	UC
		cm s^{-1}	kg m^{-3}	--- kg m^{-3} ---			--- kg m^{-3} ---		--- mm ---			---
G1	Large	13.9 ± 10.0	1287 ± 205	48 ± 1	42 ± 1	41 ± 1	1552 ± 17	2669 ± 30	14.5 ± 0.6	23.3 ± 0.8	35.4 ± 1.7	1.7 ± 0.0
G2	Medium	5.4 ± 2.5	1412 ± 180	35 ± 2	35 ± 1	36 ± 1	1683 ± 10	2620 ± 33	13.5 ± 0.1	17.5 ± 0.6	23.3 ± 0.3	1.4 ± 0.0
G3	Small	1.3 ± 0.3	1573 ± 286	25 ± 1	24 ± 2	24 ± 2	1718 ± 54	2324 ± 25	2.1 ± 0.0	9.9 ± 0.5	25.6 ± 3.6	5.6 ± 0.3

3.2 DRAINABLE POROSITY

Permeameter column drainable porosities using high compaction ranged from 34 to 50% while the jar method drainable porosities ranged from 60 to 77% (Table 3, Figure 10). The range of drainable porosity values across both the jar and permeameter methods and the permeameter compaction tests were within the range of values for woodchips reported in earlier studies. Christianson et al. (2010) and Ima and Mann (2007) reported porosities ranging from 66 to 78% and 60 to 63%, respectively, using the jar method, while Feyereisen and Christianson (2015) and Ghane et al. (2014) reported drainable porosities of 46 and 53%, respectively, using the permeameter method.

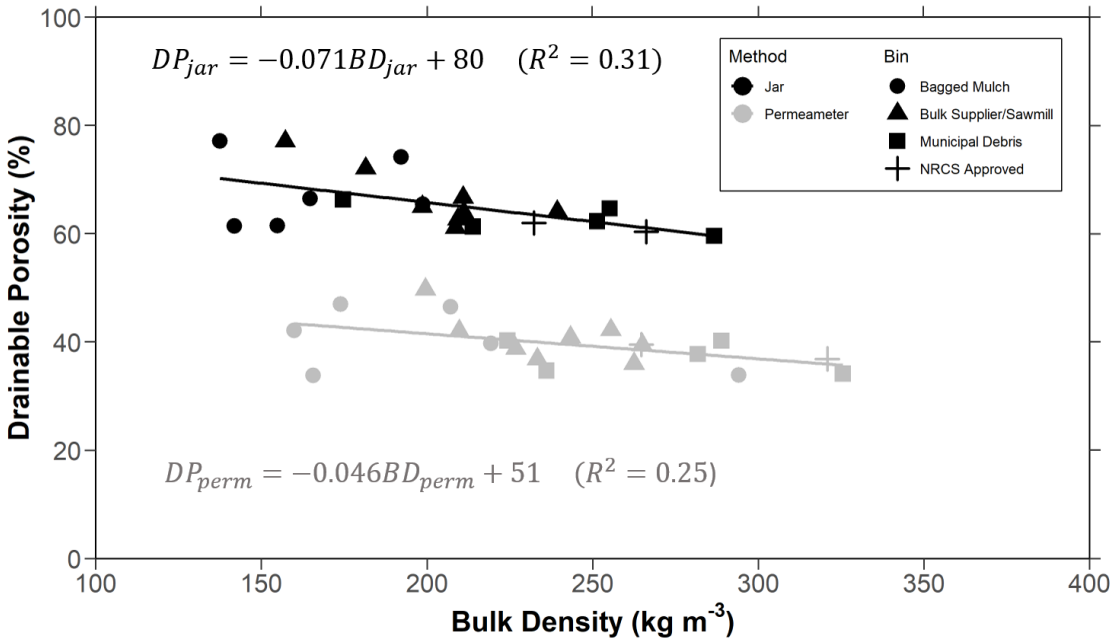

Figure 10. Scatterplots of permeameter column drainable porosity and dry bulk density with linear regression line.

The current default design value of 53% for no overburden conditions was similar to three of the four woodchip types tested under the 0 tamping conditions (Table 4). The large, relatively square NRCS approved Chips #13 and 21 and the long, shredded Chip #5 had mean drainable porosities of 54, 51, and 55%, respectively, when the permeameters were packed with no tamping. However, the current default design value of 47% for heavy overburden conditions was higher than the range of drainable porosities from the high compaction woodchip tests (25 tamps per layer). Eighteen of the twenty-one woodchip types tested had drainable porosities between 34-42% under what was likely maximum compaction (Figure 10; Table 3). Across all twenty-one woodchip types under high compaction methods, the drainable porosities averaged 40 ± 4% and had a median of 40%. It may be that the no overburden design value for drainable porosity is appropriate while the overburden design value should be decreased. However, these conclusions are contextualized within the lack of a relationship between permeameter tamping

levels to *in situ* assessment of bioreactor bulk density, especially as that relates to overburden conditions.

Many other studies have reported use of the "jar" method (e.g., Christianson et al., 2010; Ima and Mann, 2007; Niu et al., 2013; Povilaitis and Matikienė, 2020; von Ahnen et al., 2016), and comparison of the two methods here showed the jar method resulted in significantly lower compaction (p-value < 0.001) (i.e., lower bulk densities) and higher drainable porosities (p-value < 0.001) (Figure 9). These differences may be due to the difference in packing layer thickness (approximately 12 vs. 3 cm) as well as the different container size (approximately 19 vs 1 L). Regardless of method, drainable porosity decreased as bulk density increased across all woodchip types. This relationship was slightly stronger for the jar method compared to the permeameter method (R^2 of 0.31 and 0.25, respectively; Figure 10). The difference in drainable porosity between methods was consistent across woodchip types (mean ± standard deviation: 26 ± 4%, median: 26%), indicating that permeameter drainable porosity could be reasonably estimated with the jar test by subtracting 26% from jar test results. The largest difference was for Chip #9 where the jar and permeameter drainable porosities and bulk densities were 74% at 192 kg m^{-3} and 34% at 294 kg m^{-3}, respectively. The smallest difference was with Chip #4 where the jar and permeameter drainable porosities and bulk densities were 61% at 142 kg m^{-3} and 42% at 160 kg m^{-3}, respectively.

3.2.1 Total Porosity

Total porosity using the jar method ranged from 66 to 83% and was positively correlated with drainable porosity (Figure 11, $R^2 = 0.72$). However, the difference between total and drainable porosities (i.e. secondary porosity) were generally consistent across woodchip types

(mean ± standard deviation: 8 ± 3%, median: 8%) indicating that drainable porosity was the primary factor increasing total porosity. These results were comparable to Wickramarathne et al. (2020) who used similar methods and reported total porosities ranging from 61 to 74% for woodchips ranging in D_{50} from 5 to 17 mm. Other studies have found larger values with Ghane et al. (2014) and Cameron and Schipper (2012) reporting total porosities ranging from 83 to 86 and 76 to 86%, respectively, for various sizes of woodchip media.

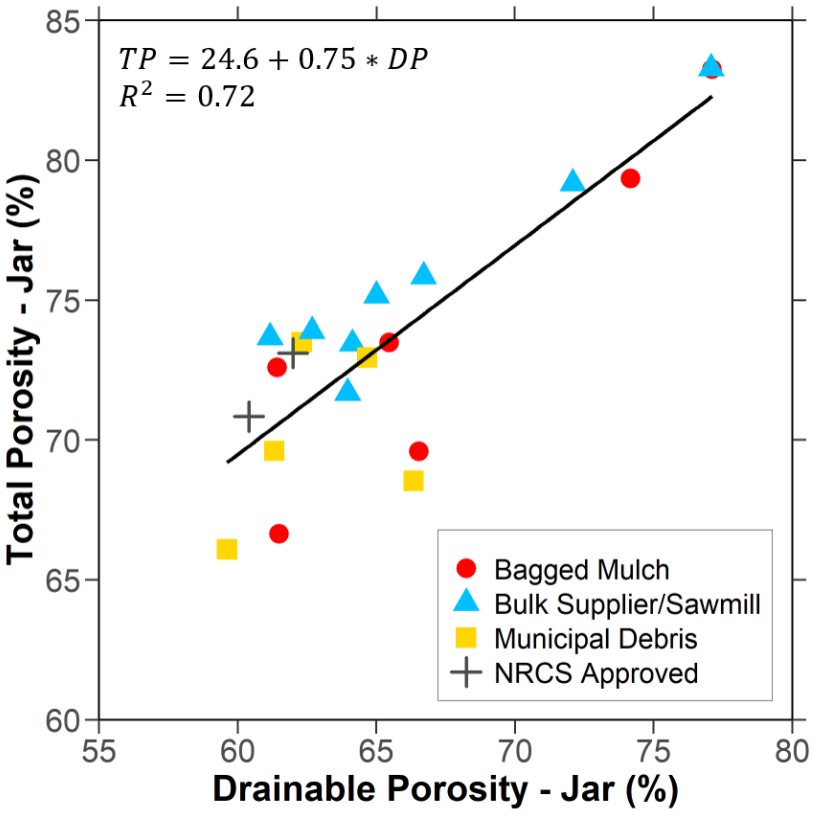

Figure 11. Scatterplot of jar method total porosity and drainable porosity. Woodchip bin indicated by point color and shape.

3.3 BULK DENSITY

Permeameter column dry bulk densities using high compaction ranged from 160 to 326 kg m^{-3}, while the jar method dry bulk densities ranged from 137 to 287 kg m^{-3} (Table 3, Figure 10). Amato et al. (2020) surveyed uncompacted cone-shaped woodchip stockpiles at wood

recycling facilities and reported bulk densities ranging from 210 to 230 kg m^{-3} for piles ranging in volume from 28.4 to 32.0 m^3. Subroy et al. (2014) estimated bulk density of woodchip stockpiles and packed laboratory containers reporting similar values of 245 ± 49 and 239 ± 38 kg m^{-3} (mean ± standard deviation) for each method, respectively. Chun et al. (2009) and Ghane et al. (2014) reported mean bulk densities of 200 and 203 kg m^{-3}, respectively, in column studies. Here, seventeen of the twenty-one woodchips tested under high compaction in the permeameter (or eleven of the twenty-one woodchips tested using the jar method) had bulk densities greater than 200 kg m^{-3}, the maximum reported in literature for packed columns. Thus, the bulk densities of many of the high compaction regime K_{sat} tests were high compared to previous literature, however few studies have reported an *in-situ* bulk density for a field bioreactor.

Permeameter bulk density significantly increased for the eight tested chip types as the number of tamps per layer increased from 0 to 10 (p-value < 0.01) (Figure 10). While bulk density continued to increase as the number of tamps per layer increased from 10 to 25 and 25 to 50, the differences were not statistically significant for most of the eight tested woodchip types (i.e. most woodchips reached maximum compaction at 10 tamps per layer). Only Chips #4 (bagged Cedar chips) and 20 (bulk shredded mulch) had statistically larger bulk densities at 25 than 10 tamps per layer (p-value = 0.041 and 0.044, respectively), while Chips #4 and 5 (bagged woodchip mulch) had statistically larger bulk densities at 50 than 25 tamps per layer (p-values = 0.024 and 0.046, respectively). These results validate the current design methods by further illustrating that compaction of woodchips increases bulk density to an extent (Figure 12), which in turn, impacts drainable porosity (Figure 8). The high compaction method of 25 tamps per layer likely resulted in relatively low K_{sat} values for the twenty-one woodchip types tested in Section 3.1.1.

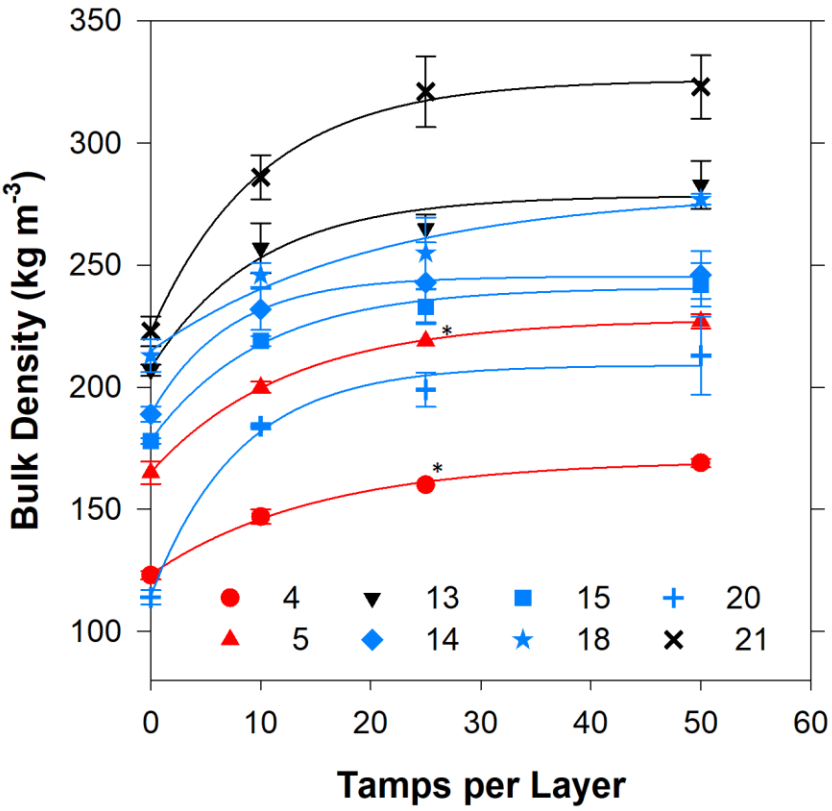

Figure 12. Change in bulk density versus permeameter tamping regime for eight selected woodchip types. Color indicates woodchip bin; black: NRCS approved, blue: bulk supplier/sawmill, red: bagged mulch. 25 tamps per layer is the ASTM standard (ASTM International, 2012a) A * indicates no error bars are shown because only one replicate is used.

3.3.1 Particle Density

Across all 21 types of woodchips, particle density ranged from 550 kg m^{-3} for Chip #4 (bagged Cedar chips) to 1030 kg m^{-3} for Chip #1 (municipal debris) with mean ± standard deviation and median of 865 ± 140 and 890 kg m^{-3}. Particle density was positively correlated with permeameter bulk density (R^2 = 0.51). Chip #4 had the lowest permeameter bulk density at high (25 tamps per layer) compaction, while Chip #1 had the fifth largest permeameter bulk density at high compaction. Thus, the differences in permeameter bulk density across woodchip types at high compaction are partially due to the differences in particle density. These results are

similar to Christianson et al. (2010) who reported particle densities ranging from 720 to 880 kg m^{-3} for a hardwood mixture.

3.4 PARTICLE SIZE

Particle size parameters D_{10}, D_{50} and UC from the sieving analysis for the twenty woodchip types excluding the Chip #7 outlier varied from 1.1 to 8.6 mm, 7.2 to 22 mm, and 2.2 to 9.5, respectively. All twenty types have smaller effective (D_{10}) and median sizes (D_{50}) than the range of 25 to 51 mm for effective size specified by the NRCS Conservation Practice Standard (USDA-NRCS, 2020), however most types had lengths within that range. This discrepancy is specifically notable for the two NRCS approved types (Chips #13 and 21) which had median sizes and median lengths of 16.1 and 13.9, and 35.6 and 42.3 mm, respectively. This shows there may be confusion around the terminology used in the standard compared to field assessment of size that an engineer may perform to approve woodchips. Mean depth, width, length, and length-to-width ratio measured by hand varied from 2.4 to 7.1, 4.7 to 22, and 23 to 52 mm, and 2.0 to 10 (Table 6, Figure 13). Manual size measurements were not normally distributed for most woodchip types, so median values were used in particle size regressions.

Table 6. Particle size parameters of all 21 types of woodchips commonly available in the U.S. Midwest region.

#	Woodchip Description	Woodchip Bin	D_{10}	D_{50}	D_{90}	UC	Length	Width	Depth	Length-to-Width Ratio	Length - Median	Width - Median	Depth - Median
			mm	mm	mm	---	mm	mm	mm	---	mm	mm	mm
1	Composting Facility Mixed Chips	Municipal Debris	7.0 ± 0.4	15.2 ± 2.2	37.1 ± 7.1	2.6 ± 0.2	34.3 ± 23.0	18.4 ± 11.5	5.9 ± 3.5	2.0 ± 1.0	24.6	15.5	4.8
2	Composting Facility Mixed Chips	Municipal Debris	3.6 ± 0.9	9.9 ± 1.5	23.4 ± 8.0	3.3 ± 0.7	31.2 ± 21.9	14.1 ± 6.8	5.8 ± 3.5	2.4 ± 1.6	22.8	13.2	4.0
3	Mixed Chips	Municipal Debris	3.1 ± 0.3	9.4 ± 0.5	27.9 ± 8.0	3.5 ± 0.1	31.6 ± 17.3	16.8 ± 8.9	6.0 ± 4.1	2.2 ± 1.2	28.6	16.1	4.8
4	Bagged Cedar Mulch	Bagged Mulch	29.4 ± 1.6	61.0 ± 10.3	84.4 ± 12.1	2.3 ± 0.3	92.1 ± 22.7	52.3 ± 17.0	14.8 ± 6.0	2.0 ± 1.1	91.8	52.9	14.5
5	Bagged Woodchip Much	Bagged Mulch	8.6 ± 0.4	22.1 ± 1.3	42.1 ± 6.6	3.0 ± 0.2	44.0 ± 24.8	21.4 ± 13.4	5.7 ± 3.3	2.6 ± 1.8	35.7	16.9	5.1
6	Bagged Cypress Mulch	Bagged Mulch	2.4 ± 0.2	7.2 ± 0.5	17.9 ± 0.9	3.9 ± 0.2	40.5 ± 20.6	7.2 ± 3.6	3.9 ± 2.2	6.3 ± 3.1	33.0	5.6	3.5
7	Bagged Pine Bark Mulch	Bagged Mulch	2.2 ± 0.1	7.4 ± 1.3	21.8 ± 3.1	4.4 ± 0.4	43.5 ± 19.1	5.3 ± 2.6	3.0 ± 2.0	9.1 ± 4.4	39.8	4.6	2.6
8	Bagged Shredded Cedar Mulch	Bagged Mulch	2.6 ± 0.1	10.2 ± 0.4	21.6 ± 1.8	4.9 ± 0.3	29.0 ± 17.3	4.7 ± 3.5	2.4 ± 2.3	7.5 ± 4.8	25.9	3.8	1.8
9	Bagged Hardwood Mulch	Bagged Mulch	1.1 ± 0.2	7.3 ± 2.4	29.0 ± 9.3	9.5 ± 1.7	31.7 ± 20.1	5.1 ± 3.8	2.7 ± 2.0	8.3 ± 6.7	21.0	4.1	2.2
10	Municipal Tree Debris Mixed Chips	Municipal Debris	7.1 ± 0.1	15.9 ± 1.3	37.2 ± 6.2	2.7 ± 0.3	31.8 ± 15.1	11.6 ± 5.9	7.1 ± 4.1	3.3 ± 2.2	29.2	10.8	7.3

Table 6 (cont.)

#	Woodchip Description	Woodchip Bin	D_{10} mm	D_{50} mm	D_{90} mm	UC ---	Length mm	Width mm	Depth mm	Length-to-Width Ratio ---	Length - Median mm	Width - Median mm	Depth - Median mm
11	Composting Facility Mixed Hardwood Chips	Bulk Supplier/Sawmill	3.8 ± 0.5	9.7 ± 0.3	18.9 ± 3.2	2.9 ± 0.5	33.9 ± 25.2	8.5 ± 4.2	3.6 ± 1.8	4.6 ± 3.5	24.8	6.8	3.1
12	Composting Facility Mixed Hardwood Chips	Bulk Supplier/Sawmill	5.6 ± 1.3	12.6 ± 1.8	32.6 ± 6.7	2.8 ± 0.5	45.7 ± 29.2	18.2 ± 15.3	5.4 ± 3.0	4.0 ± 4.6	35.3	13.3	4.6
13	Maple-Oak Mixed Chips (NRCS spec)	NRCS Approved	8.1 ± 0.8	16.1 ± 0.7	29.2 ± 2.6	2.2 ± 0.2	44.4 ± 27.1	22.3 ± 9.2	6.3 ± 3.0	2.5 ± 2.5	35.6	21.5	5.4
14	Mixed Hardwood Chips	Bulk Supplier/Sawmill	5.2 ± 1.1	11.7 ± 0.7	26.1 ± 7.7	2.7 ± 0.3	33.1 ± 13.3	17.6 ± 7.7	5.2 ± 2.9	2.1 ± 0.8	31.0	16.7	4.2
15	Bagged Hardwood Playground Chips	Bulk Supplier/Sawmill	2.4 ± 0.2	8.8 ± 0.0	13.2 ± 1.0	4.1 ± 0.3	23.4 ± 12.6	6.3 ± 3.0	3.0 ± 1.9	4.1 ± 1.9	21.7	5.9	2.7
16	Municipal Mixed Oak Chips	Bulk Supplier/Sawmill	6.5 ± 0.5	13.5 ± 0.8	26.5 ± 4.6	2.4 ± 0.1	31.5 ± 24.9	15.2 ± 7.1	4.4 ± 2.0	2.3 ± 1.8	24.3	14.1	4.3
17	Municipal Tree Debris Mixed Chips (Derecho)	Municipal Debris	6.3 ± 0.6	12.9 ± 2.0	28.2 ± 3.2	2.3 ± 0.2	32.3 ± 22.3	12.7 ± 7.7	4.0 ± 2.3	3.4 ± 3.2	24.1	11.4	3.9
18	Mixed Hardwood Chips	Bulk Supplier/Sawmill	7.2 ± 0.6	16.8 ± 0.7	33.8 ± 2.0	2.7 ± 0.4	36.1 ± 19.2	15.2 ± 7.0	6.6 ± 4.0	2.7 ± 1.8	29.6	14.0	5.6

Table 6 (cont.)

#	Woodchip Description	Woodchip Bin	D_{10}	D_{50}	D_{90}	UC	Length	Width	Depth	Length-to-Width Ratio	Length - Median	Width - Median	Depth - Median
			mm	mm	mm	---	mm	mm	mm	---	mm	mm	mm
19	Mixed Softwood Chips	Bulk Supplier/Sawmill	7.2 ± 0.8	17.5 ± 1.0	36.4 ± 3.0	2.9 ± 0.1	47.5 ± 21.7	16.3 ± 8.0	5.4 ± 2.3	3.7 ± 2.3	42.0	15.3	5.4
20	Mixed Shredded Mulch	Bulk Supplier/Sawmill	3.6 ± 0.4	12.1 ± 0.5	26.0 ± 4.6	4.0 ± 0.6	51.8 ± 24.5	6.3 ± 3.5	3.4 ± 2.4	10.5 ± 7.2	46.5	5.60	2.80
21	Mixed Hardwood Chips (NRCS spec)	NRCS Approved	5.3 ± 0.5	13.9 ± 2.0	28.5 ± 4.5	3.1 ± 0.2	47.3 ± 21.4	16.1 ± 6.7	6.4 ± 3.1	3.7 ± 3.2	42.2	15.0	5.60

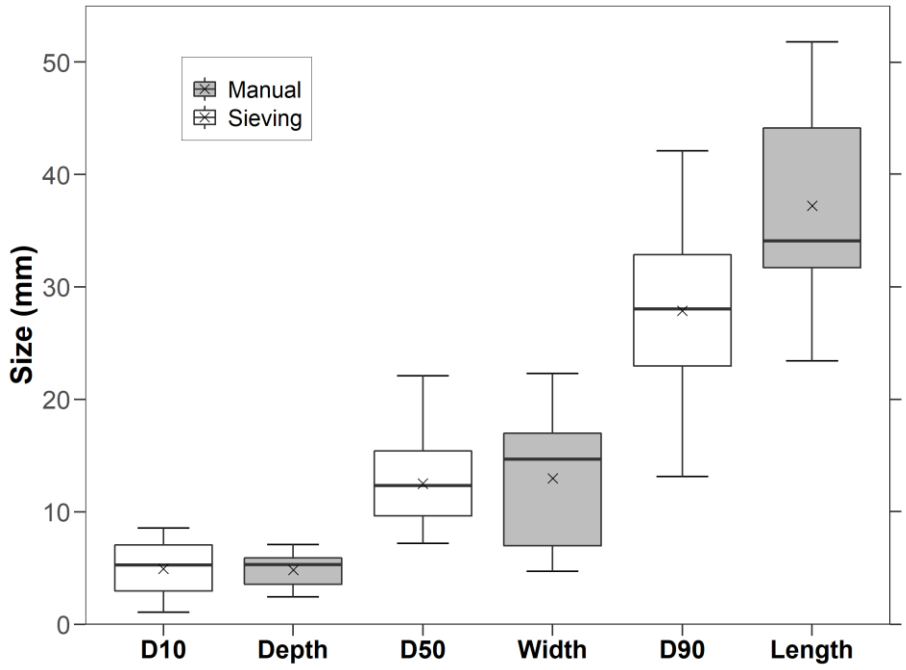

Figure 13. Boxplots of sieve-test derived D_{10}, D_{50}, and D_{90}, and manually measured median depth, width, and length of all woodchip types except the outlier Chip #7. Boxes, stems, and dots represent the 25th and 75th, 10th and 90th, and 5th and 95th percentiles, respectively; the horizontal line is the median, and the x is the mean.

It is desirable to estimate properties that are laborious to measure (i.e. K_{sat}) from easier-to-measure properties (i.e. particle size) to streamline bioreactor woodchip suitability assessments in the field. The multiple linear regression indicated the median woodchip width was important given the drainable porosity was known (or could be estimated, see section 3.2). Median woodchip width was most strongly positively correlated with D_{10} (correlation coefficient, r = 0.79) and strongly negatively correlated with the uniformity coefficient (r = -0.820; Figure 12). Manually measuring woodchip width requires a sufficiently high population for a representative sample and is not recommended in the field.

The strongest correlations between manually measured and sieve method particle size measurements were the manually measured median woodchip width and depth parameters with the D_{10}, D_{50}, D_{90} (Figure 14). Manually measured median woodchip length did not exhibit a

strong correlation with any particle size parameter (Figure 14). Uniformity coefficient was strongly positively correlated with length-to-width ratio (r = 0.98) and negatively correlated with manually measured width and depth (r = -0.82 and -0.69, respectively).

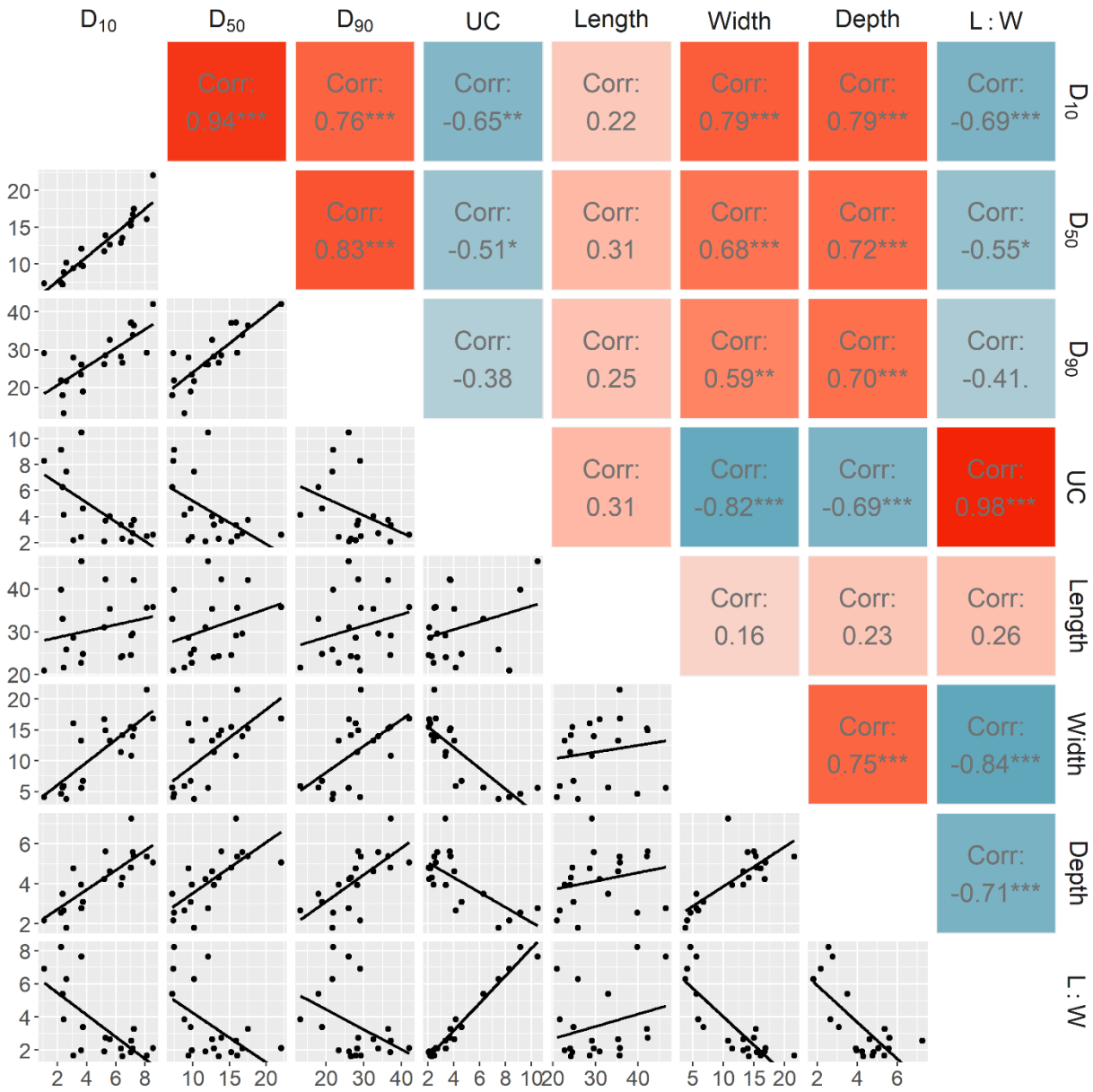

Figure 14. Scatterplot matrix of particle size parameters D_{10} (effective size), D_{50} (median size), D_{90} (90% smaller by mass size), UC (uniformity coefficient), Length (median manually measured length), Width (median manually measured width), Depth (median manually measured depth), and L:W (median manually measured length-to-width ratio). Upper triangle boxes display correlation coefficients (r) with darker colors indicating stronger correlations; red and blue indicate positive and negative correlations, respectively. Significance levels: *** = p-value < 0.001, ** = p-value < 0.01, * = p-value <0.05, "." = p-value < 0.10.

3.5 NUTRIENT ANALYSIS

All woodchip types were similar in carbon content (coefficient of variation = 0.036), but there was greater variability in nitrogen and phosphorous content (coefficient of variations = 0.49 and 0.83, respectively). Eighteen of the twenty-one woodchip carbon contents were in the range of approximately 46 to 49 %C (n = 21, mean 47.4 ± 1.7%; median 47.8 %C). Chip #21, which met NRCS specifications for field bioreactor installation, was notably low at 43.7 %C; this wood consisted of primarily Hickory and Maple. The pine bark (Chip #7) had the highest carbon content of 50.9%. It is well established that bark wood is chemically distinct from heart/sapwood, with the former having higher nutrient contents (Koch 1985).

Table 7. Nutrient content and carbon to nitrogen ratio of all 21 woodchip types commonly available in the U.S. Midwest Region. Values with no standard deviation had only one replicate above the minimum detection threshold.

#	Woodchip Description	Woodchip Bin	Carbon	Nitrogen	Phosphorus	C/N ratio
			%	%	%	---
1	Composting Facility Mixed Chips	Municipal Debris	46.6 ± 0.2	0.41 ± 0.04	0.023 ± 0.002	113 ± 10
2	Composting Facility Mixed Chips	Municipal Debris	45.6 ± 0.1	0.45 ± 0.03	0.017 ± 0.001	102 ± 7
3	Mixed Chips	Municipal Debris	47.5 ± 0.2	0.42 ± 0.02	0.026 ± 0.002	114 ± 5
4	Bagged Cedar Mulch	Bagged Mulch	49.1 ± 0.3	0.24 ± 0.04	0.011	211
5	Bagged Woodchip Much	Bagged Mulch	48.7 ± 0.0	0.21	<0.010	232
6	Bagged Cypress Mulch	Bagged Mulch	49.2 ± 0.3	<0.20	<0.010	>246
7	Bagged Pine Bark Mulch	Bagged Mulch	50.9 ± 0.3	0.22 ± 0.01	0.015 ± 0.001	237
8	Bagged Shredded Cedar Mulch	Bagged Mulch	48.0 ± 0.2	0.28 ± 0.02	0.011 ± 0.001	172 ± 13
9	Bagged Hardwood Mulch	Bagged Mulch	45.0 ± 0.7	0.47 ± 0.05	0.015 ± 0.002	97 ± 13
10	Municipal Tree Debris Mixed Chips	Municipal Debris	45.8 ± 0.4	0.86 ± 0.10	0.087 ± 0.004	54 ± 6
11	Composting Facility Mixed Hardwood Chips	Bulk Supplier/Sawmill	44.7 ± 1.9	0.64 ± 0.17	0.059 ± 0.006	72 ± 15

Table 7 (cont.)

#	Woodchip Description	Woodchip Bin	Carbon	Nitrogen	Phosphorus	C/N ratio
			%	%	%	---
12	Composting Facility Mixed Hardwood Chips	Bulk Supplier/Sawmill	46.6 ± 0.4	0.54 ± 0.06	0.039 ± 0.003	88 ± 11
13	Maple-Oak Mixed Chips (NRCS spec)	NRCS Approved	47.5 ± 0.2	0.37 ± 0.02	0.022 ± 0.001	127 ± 7
14	Mixed Hardwood Chips	Bulk Supplier/Sawmill	48.0 ± 0.2	0.24 ± 0.02	0.014 ± 0.001	201 ± 14
15	Bagged Hardwood Playground Chips	Bulk Supplier/Sawmill	48.2 ± 0.2	0.24 ± 0.04	0.015 ± 0.002	203 ± 26
16	Municipal Mixed Oak Chips	Bulk Supplier/Sawmill	48.4 ± 0.3	0.22 ± 0.02	0.016	224 ± 16
17	Municipal Tree Debris Mixed Chips (Derecho)	Municipal Debris	46.6 ± 0.0	0.43 ± 0.02	0.037 ± 0.002	108 ± 5
18	Mixed Hardwood Chips	Bulk Supplier/Sawmill	47.8 ± 0.1	0.28 ± 0.01	0.016 ± 0.002	173 ± 6
19	Mixed Softwood Chips	Bulk Supplier/Sawmill	48.8 ± 0.1	0.26 ± 0.04	0.013 ± 0.001	187 ± 24
20	Mixed Shredded Mulch	Bulk Supplier/Sawmill	48.4 ± 0.4	0.23 ± 0.02	0.013 ± 0.003	211 ± 20
21	Mixed Hardwood Chips (NRCS spec)	NRCS Approved	43.7 ± 2.2	0.21 ± 0.01	0.015 ± 0.001	212 ± 14

The relatively greater range of nitrogen content (0.20 to 0.86 %N) compared to carbon drove the notable differences in C:N ratio across the woods tested here. The lowest C:N of 53:1 was associated with Chip #10, a municipal debris. This woodchip had the highest nitrogen and phosphorus contents (0.86 %N and 0.087 %P) which matched observations that it contained noticeable amounts of leaves. Woodchips from bioreactor installations and recharges (Chips #3, 13, 18, and 21) had C:N ratios ranging from 114:1 to 212:1, which is lower than in some studies but within the range of 30:1 to 300:1 generally reported for wood media (Christianson et al., 2010; Greenan et al., 2006; Schipper et al., 2010).

Woodchip P content was strongly positively correlated with N content and negatively correlated with C:N ratio (Figure 13). The bagged mulch and bulk supplier/sawmill bins

contained woodchips with the highest C content and C:N ratio. The two NRCS approved chips contained 43.7 and 47.5 %C and C:N ratios of 127:1 and 212:1. Municipal debris chips were generally lower in C:N ratio than other bins and included the lowest C:N ratio (Chip #10), but bagged mulch and bulk supplier/sawmill chips also included chips with low C:N ratios ranging from 72:1 to 97:1.

These results must be considered with the physical and hydraulic properties of the wood media as nutrient content is central to the denitrification process. Carbon media with improper nutrient content could contribute to pollution swapping with P, biochemical oxygen demand, or greenhouse gases (Christianson et al. 2017, Healy et al. 2012, Schipper et al. 2010).

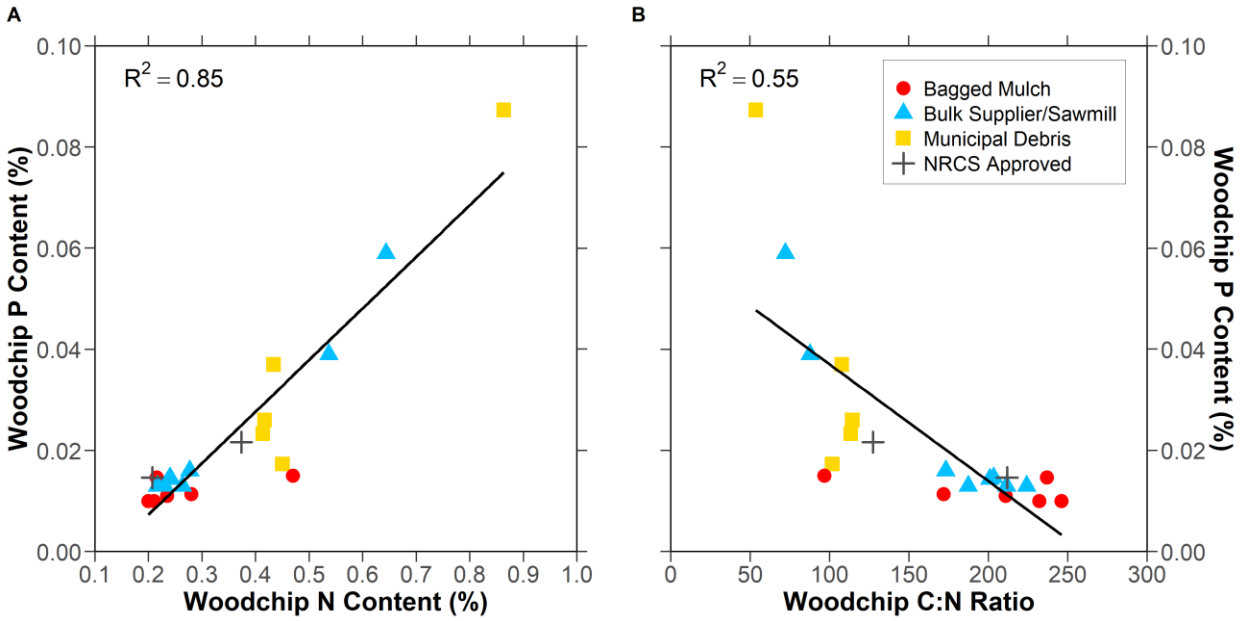

Figure 15. Linear regression of woodchip phosphorus content with nitrogen content (A) and carbon to nitrogen ratio (B).

CHAPTER 4: CONCLUSIONS

High compaction procedures adapted from a standard method for soils limited the range and magnitude of K_{sat} values across 20 woodchip types commonly available in the U.S. Midwest region to 0.10 to 2.05 cm s^{-1}. Reduced compaction produced higher K_{sat} and drainable porosity values (2.07 to 7.44 cm s^{-1} and 41 to 55%, respectively) for three larger woodchip types, similar to prior studies and current practice standards. Multiple (R^2 of 0.48) and single (R^2s of 0.31 and 0.25) linear regression analysis confirmed the hypothesis that saturated hydraulic conductivity was positively correlated with drainable porosity and particle size (median width and D_{50}), although these models were constrained by the small range of K_{sat} values under the high compaction method. Drainable porosity decreased as bulk density increased across woodchip types using both the jar and permeameter methods. This relationship was more prominent when comparing reduced compaction with high compaction results.

It was hypothesized that manually measured woodchip sizes would be more related to K_{sat} than sieve method parameters, however this was only true in the multiple linear regression model. Using discrete single parameter regressions, woodchip median diameter (D_{50}) was the particle size parameter most strongly correlated with K_{sat} (R^2 = 0.25). Nearly all of the woodchips tested (20 of 21) had a smaller D_{50} than the recommended effective diameter (D_{10}) specified by the NRCS Conservation Practice Standard of 25 to 51 mm. Despite having sizes smaller than design guidelines, three of the woodchips tested at reduced compaction exhibited K_{sat} values (6.13, 7.44, and 5.87 cm s^{-1}) larger than practice standard recommendations of 2.94 cm s^{-1} for non-overburden conditions.

These results demonstrated the high sensitivity of woodchip K_{sat} and porosity to compaction (i.e. bulk density), verifying some aspects of current design methods but also

providing guidance to improve current practice standards. The current drainable porosity default design value of 53% for no overburden conditions was similar to woodchips tested under the 0 tamping conditions, whereas the default value of 47% for heavy overburden conditions was higher than most of the woodchips when tested under high compaction (25 tamps per layer; drainable porosity mean 40 ± 4%). Therefore, the drainable porosity design value for overburden conditions may need to be adjusted lower than 47%, however this is contingent upon better estimation of *in situ* bulk density to relate to laboratory compaction.

This work demonstrated that most current field bioreactor studies are missing a crucial component: measurement of *in situ* bulk density. It is difficult to make specific recommendations for K_{sat} and porosity design values due to the inability to compare laboratory bulk density values with *in situ* bulk density. Thus, it is recommended that further studies continue to investigate the effects of overburden by measuring K_{sat} of more woodchip types at reduced compaction levels, measuring K_{sat} and porosity under sustained overburden conditions (in contrast to packed chips), and by pairing laboratory measurements with *in situ* measurements of bulk density, porosity, and K_{sat}.

REFERENCES

Amato, M. T., Giménez, D., Kannepalli, S., Strom, P. F., Krogmann, U., & Miskewitz, R. J. (2020). Forecasting leachate generation from pilot woodchip stockpiles using a three-dimensional transient flow model. *J. Environ. Manage., 262*, 110379. doi:https://doi.org/10.1016/j.jenvman.2020.110379

ANSI/ASABE. (1992). S424.1: Method of determining and expressing particle size of chopped forage materials by screening. St. Joseph, MI: ASABE

ASTM. (2012). D1557: Standard test methods for laboratory compaction characteristics of soil using modified effort. West Conshohocken, PA: ASTM Int.

ASTM. (2019). D2343: Standard test method for permeability of granular soils (constant head). West Conshohocken, PA: ASTM Int.

Blowes, D. W., Robertson, W. D., Ptacek, C. J., & Merkley, C. (1994). Removal of agricultural nitrate from tile-drainage effluent water using in-line bioreactors. *J. Contam. Hydrol*, *15*, 207-221. https://doi.org/10.1016/0169-7722(94)90025-6

Bordier, C., & Zimmer, D. (2000). Drainage equations and non-Darcian modelling in coarse porous media or geosynthetic materials. *J. Hydrol.*, *228*(3), 174-187. doi:https://doi.org/10.1016/S0022-1694(00)00151-7

Burbery, L. F., Abraham, P., & Afrit, B. (2014). Determining the hydraulic properties of wood/gravel mixtures for use in denitrifying walls. *J. Hydrol. (NZ), 53*(1), 1-21.

Cameron, S. G., & Schipper, L. A. (2010). Nitrate removal and hydraulic performance of organic carbon for use in denitrification beds. *Ecol. Eng., 36*(11), 1588-1595. doi:https://doi.org/10.1016/j.ecoleng.2010.03.010

Cameron, S. G., & Schipper, L. A. (2012). Hydraulic properties, hydraulic efficiency and nitrate removal of organic carbon media for use in denitrification beds. *Ecol. Eng., 41*, 1-7. doi:https://doi.org/10.1016/j.ecoleng.2011.11.004

Christianson, L., Castello, A., Christianson, R., Helmers, M., & Bhandari, A. (2010). Hydraulic property determination of denitrifying bioreactor fill media. *Appl. Eng. Agric., 26*(5), 849-854. https://doi.org/10.13031/2013.34946

Christianson, L. E., Bhandari, A., & Helmers, M. J. (2012). A practice-oriented review of woodchip bioreactors for subsurface agricultural drainage. *Appl. Eng. Agric., 28*(6), 861-874. doi:https://doi.org/10.13031/2013.42479

Christianson, L. E., Lepine, C., Sibrell, P. L., Penn, C., & Summerfelt, S. T. (2017). Denitrifying woodchip bioreactor and phosphorus filter pairing to minimize pollution swapping. *Water Res., 121*, 129-139. doi:https://doi.org/10.1016/j.watres.2017.05.026

Chun, J. A., Cooke, R. A., Eheart, J. W., & Kang, M. S. (2009). Estimation of flow and transport parameters for woodchip-based bioreactors: I. Laboratory-scale bioreactor. *Biosys. Eng., 104*(3), 384-395. doi:https://doi.org/10.1016/j.biosystemseng.2009.06.021

Cooke, R. A., & Bell, N. L. (2014). Protocol and interactive routine for the design of subsurface bioreactors. *Appl. Eng. Agric., 30*(5), 761-771. doi:https://doi.org/10.13031/aea.30.9900

Cooke, R. A., M. Doheny, A., & C. Hirschi, M. (2001). Bio-reactors for edge-of-field treatment of tile outflow. ASABE Paper No. 012018. St. Joseph, MI: ASABE.

de Mendiburu, F. (2020). Agricolae: Statistical procedures for agricultural research (Version 1.3-3.). Retrieved from https://CRAN.R-project.org/package=agricolae

Dinnes, D. L., Karlen, D. L., Jaynes, D. B., Kaspar, T. C., Hatfield, J. L., Colvin, T. S., & Cambardella, C. A. (2002). Nitrogen management strategies to reduce nitrate leaching in tile-drained Midwestern soils. *Agron. J., 94*(1), 153-171. doi:10.2134/agronj2002.1530

Fetter, C. W. (2001). *Applied hydrogeology* (P. Lynch Ed. Fourth ed.). Upper Saddle River, New Jersey: Prentice-Hall, Inc.

Feyereisen, G. W., & Christianson, L. E. (2015). Hydraulic flow characteristics of agricultural residues for denitrifying bioreactor media. *Appl. Eng. Agric., 31*(1), 89-96. doi:10.13031/aea.31.10552

Ghane, E., Fausey, N. R., & Brown, L. C. (2014). Non-Darcy flow of water through woodchip media. *J. Hydrol., 519*, 3400-3409. doi:https://doi.org/10.1016/j.jhydrol.2014.09.065

Ghane, E., Feyereisen, G. W., & Rosen, C. J. (2016). Non-linear hydraulic properties of woodchips necessary to design denitrification beds. *J. Hydrol., 542*, 463-473. doi:https://doi.org/10.1016/j.jhydrol.2016.09.021

Greenan, C. M., Moorman, T. B., Kaspar, T. C., Parkin, T. B., & Jaynes, D. B. (2006). Comparing carbon substrates for denitrification of subsurface drainage water. *J. Environ. Qual., 35*(3), 824-829. doi:10.2134/jeq2005.0247

Gupta, R. S. (2017). *Hydrology and hydraulic systems* (Fourth ed.). Long Grove, Illinois: Waveland Press, Inc.

Hair, J. F., Jr, Black, W. C., Babin, B. J., & Anderson, R. E. (2009). *Multivariate data analysis* (7th ed.): Pearson.

Healy, M. G., Ibrahim, T. G., Lanigan, G. J., Serrenho, A. J., & Fenton, O. (2012). Nitrate removal rate, efficiency and pollution swapping potential of different organic carbon media in laboratory denitrification bioreactors. *Ecol. Eng., 40*, 198-209. doi:https://doi.org/10.1016/j.ecoleng.2011.12.010

Hebbali, A. (2020). Olsrr: Tools for building OLS regression models. (Version 0.5.3). Retrieved from https://CRAN.R-project.org/package=olsrr

Hogg, R. V., Tanis, E. A., & Zimmerman, D. L. (2015). *Probability and Statistical Inference* (9th ed.): Pearson Education, Inc.

Illinois NRCS. (2021). G605-1: Conservation practice guidance 605 - Denitrifying bioreactor. Champaign, IL: NRCS, Illinois.

Ima, C. S., & Mann, D. (2007). Physical Properties of Woodchip: Compost Mixtures used as Biofilter Media. *Agric. Eng. Int.: The CIGR Journal*.

Judge, A. (2013). Measurement of the hydraulic conductivity of gravels using a laboratory permeameter and silty sands using field testing with observation wells. PhD diss. Amherst, Massachusetts: University of Massachusetts Amherst.

Mississippi River/Gulf of Mexico Watershed Nutrient Task Force. (2001). *Action Plan for Reducing, Mitigating, and Controlling Hypoxia in the Northern Gulf of Mexico*. Washington, DC.

Niu, S., Guerra, H. B., Chen, Y., Park, K., & Kim, Y. (2013). Performance of a vertical subsurface flow (VSF) wetland treatment system using woodchips to treat livestock stormwater. *Environ Sci: Process. & Impacts, 15*(8), 1553-1561. doi:10.1039/C3EM00107E

Povilaitis, A., & Matikienė, J. (2020). Nitrate removal from tile drainage water: The performance of denitrifying woodchip bioreactors amended with activated carbon and flaxseed cake. *Agric. Water Manage., 229*, 105937. doi:https://doi.org/10.1016/j.agwat.2019.105937

R Core Team. (2020). R: A language and computing environment for statistical computing: R Foundation for Statistical Computing, Vienna, Austria.

Rabalais, N. N., Turner, R. E., Justić, D., Dortch, Q., Wiseman, W. J., & Sen Gupta, B. K. (1996). Nutrient changes in the Mississippi River and system responses on the adjacent continental shelf. *Estuaries, 19*(2), 386-407. doi:10.2307/1352458

Rabalais, N. N., Turner, R. E., & Scavia, D. (2002). Beyond science into policy: Gulf of Mexico hypoxia and the Mississippi River: Nutrient policy development for the Mississippi River watershed reflects the accumulated scientific evidence that the increase in nitrogen

loading is the primary factor in the worsening of hypoxia in the northern Gulf of Mexico. *Bioscience, 52*(2), 129-142. doi:10.1641/0006-3568(2002)052[0129:Bsipgo]2.0.Co;2

Robertson, W., & Merkley, C. (2009). In-stream bioreactor for agricultural nitrate treatment. *J. Environ. Qual., 38*, 230-237. doi:10.2134/jeq2008.0100

Schipper, L. A., Robertson, W. D., Gold, A. J., Jaynes, D. B., & Cameron, S. C. (2010). Denitrifying bioreactors—An approach for reducing nitrate loads to receiving waters. *Ecol. Eng., 36*(11), 1532-1543. doi:https://doi.org/10.1016/j.ecoleng.2010.04.008

Subroy, V., Giménez, D., Qin, M., Krogmann, U., Strom, P. F., & Miskewitz, R. J. (2014). Hydraulic properties of coarsely and finely ground woodchips. *J. Hydrol., 517*, 201-212. doi:https://doi.org/10.1016/j.jhydrol.2014.05.025

USDA-NRCS. (2019). Denitrifying Bioreactor Design (Version 1.9) [Excel file]. Retrieved from https://www.nrcs.usda.gov/wps/cmis_proxy/https/ecm.nrcs.usda.gov%3a443/fncmis/resources/WEBP/ContentStream/idd_A04CDA69-0000-C61C-8ABC-065BFF16A92D/0/ILSS11Bioreactor_v1.9.xlsb

USDA-NRCS. (2020). 605-CPS-1: Denitrifying bioreactor. Washington, D.C: USDA-NRCS.

van Driel, P. W., Robertson, W. D., & Merkley, L. C. (2006). Denitrification of agricultural drainage using wood-based reactors. *Trans. ASABE, 49*(2), 565-573.

von Ahnen, M., Pedersen, P. B., & Dalsgaard, J. (2016). Start-up performance of a woodchip bioreactor operated end-of-pipe at a commercial fish farm—A case study. *Aquacult. Eng., 74*, 96-104. doi:https://doi.org/10.1016/j.aquaeng.2016.07.002

Wickramarathne, N. M., Cooke, R. A., Book, R., & Christianson, L. E. (2020). Denitrifying woodchip bioreactor leachate tannic acid and true color: Lab and field studies. *Trans. ASABE, 63*(6), 1747-1757. doi:https://doi.org/10.13031/trans.14020

APPENDIX A: SUPPLEMENTARY WOODCHIP INFORMATION

Chip #1 – UIUC F&S Mix 1
Description: Composting facility mixed chips, light colored, mainly square-shaped particles
Source or Supplier: University of Illinois Urbana-Champaign Facilities and Services Composting Facility

Figure 16. Close-up photograph of Chip #1 with scale in centimeters.

Figure 17. Large-scale photograph of Chip #1 depicting visual size distribution. Ruler top and bottom gradations in inches and centimeters, respectively.

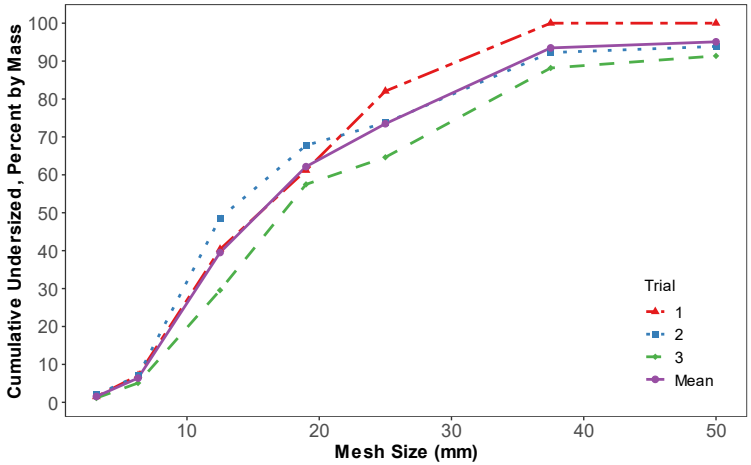

Figure 18. Particle size distribution of Chip #1, three repetitions and mean

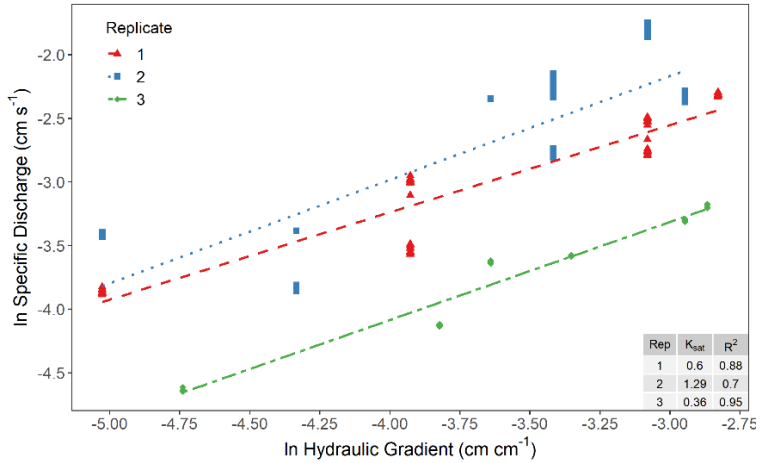

Figure 19. Saturated hydraulic conductivity calculation from regression of natural log corrected specific discharge and hydraulic gradient data for Chip #1. Viscosity-adjusted K_{sat} values used for mean calculation shown in inset table.

Chip #2 – UIUC F&S Mix 2
Description: Composting facility mixed chips, visually darker than Chip 1 mainly square-shaped particles, appeared to have more small pieces than Chip 1.
Source or Supplier: University of Illinois Urbana-Champaign Facilities and Services Composting Facility

Figure 20. Close-up photograph of Chip #2 with scale in centimeters.

Figure 21. Large-scale photograph of Chip #2 depicting visual size distribution. Ruler top and bottom gradations in inches and centimeters, respectively.

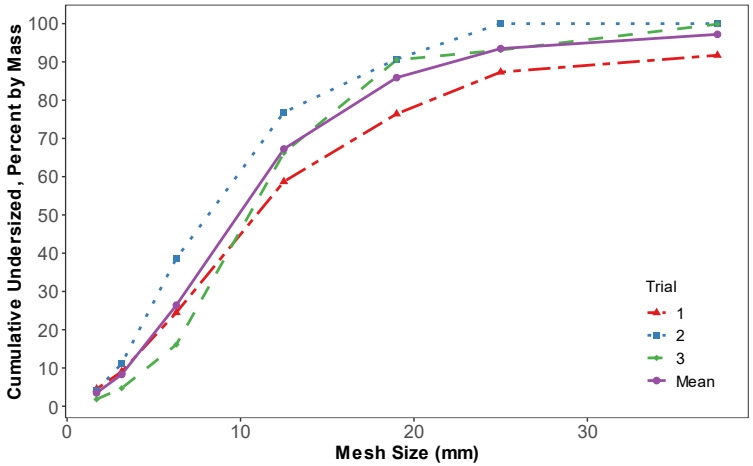

Figure 22. Particle size distribution of Chip #2, three repetitions and mean.

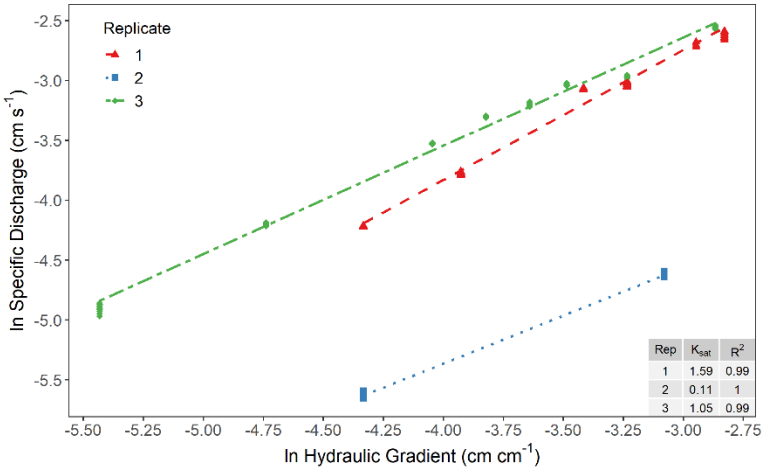

Figure 23. Saturated hydraulic conductivity calculation from regression of natural log corrected specific discharge and hydraulic gradient data for Chip #2. Viscosity-adjusted K_{sat} values used for mean calculation shown in inset table.

Chip #3 – UIUC AgEng Farm Bioreactor Recharge Chips
Description: Mixed chips, included pine needles (likely softwood mix), mainly square-shaped particles with some long stick pieces.
Source or Supplier: University of Illinois Urbana-Champaign Agricultural Engineering Farm Bioreactor Recharge

Figure 24. Close-up photograph of Chip #3 with scale in centimeters.

Figure 25. Large-scale photograph of Chip #3 depicting visual size distribution. Ruler top and bottom gradations in inches and centimeters, respectively.

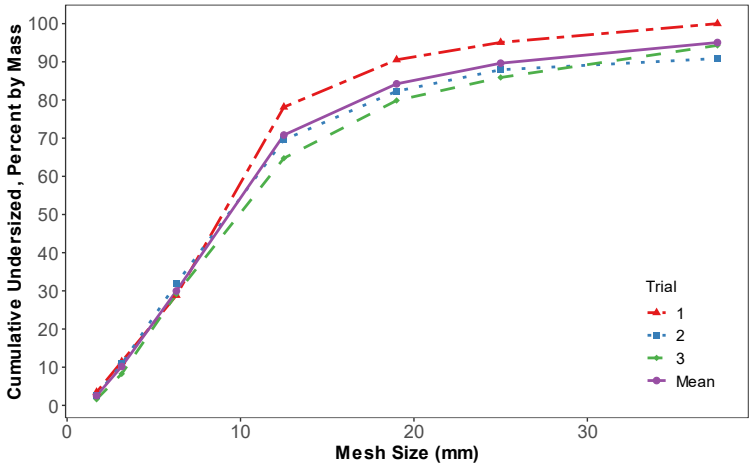

Figure 26. Particle size distribution of Chip #3, three repetitions and mean.

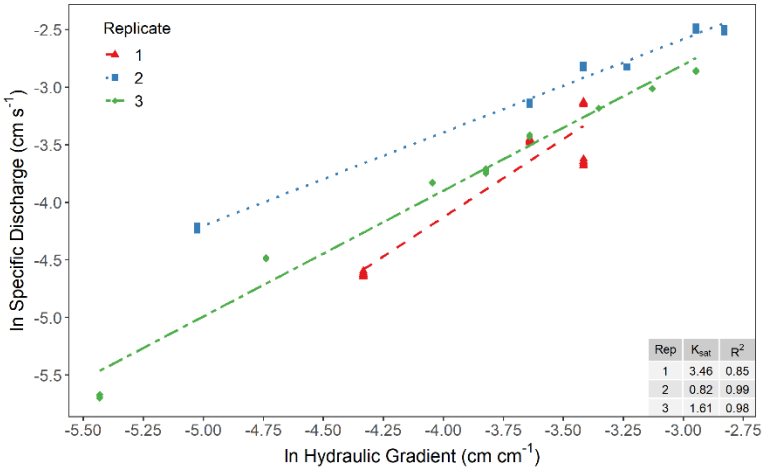

Figure 27. Saturated hydraulic conductivity calculation from regression of natural log corrected specific discharge and hydraulic gradient data for Chip #3. Viscosity-adjusted K_{sat} values used for mean calculation shown in inset table.

Chip #4 – Cedar Chips
Description: Bagged cedar chips mulch, mainly square-shaped particles
Source or Supplier: Lowes, Champaign, IL

Figure 28. Close-up photograph of Chip #4 with scale in centimeters.

Figure 29. Large-scale photograph of Chip #4 depicting visual size distribution. Ruler top and bottom gradations in inches and centimeters, respectively.

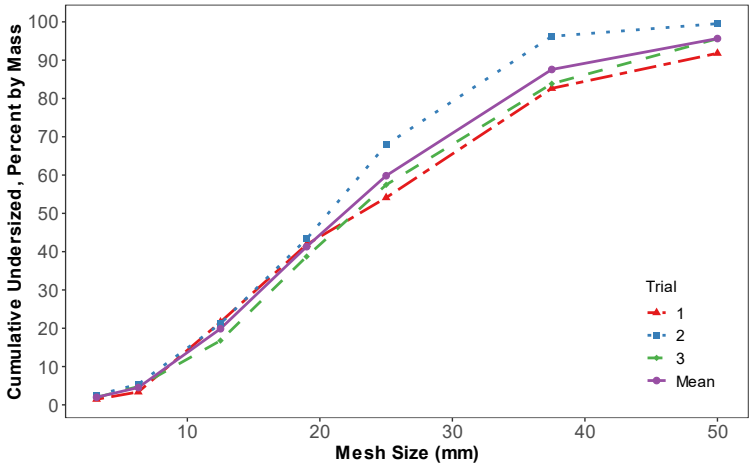

Figure 30. Particle size distribution of Chip #4, three repetitions and mean.

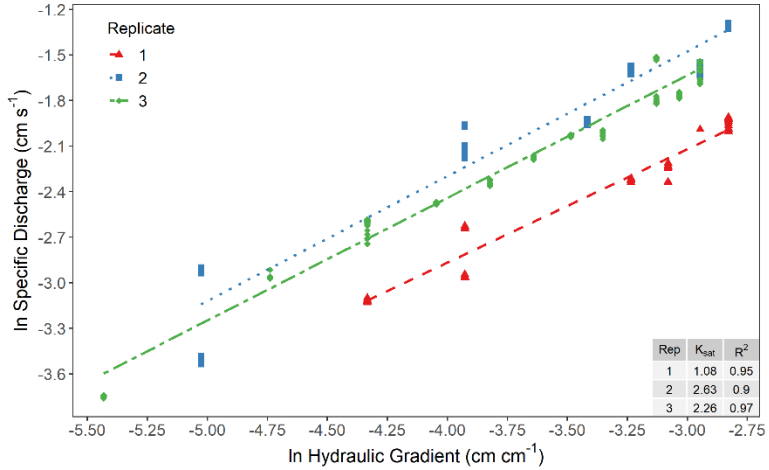

Figure 31. Saturated hydraulic conductivity calculation from regression of natural log corrected specific discharge and hydraulic gradient data for Chip #4. Viscosity-adjusted K_{sat} values used for mean calculation shown in inset table.

Chip #5 – Recycled Wood Woodchip Mulch
Description: Bagged woodchip mulch; mix of shredded and chipped, mainly long and narrow particles
Source or Supplier: Menards, Champaign, IL

Figure 32. Close-up photograph of Chip #5 with scale in centimeters.

Figure 33. Large-scale photograph of Chip #5 depicting visual size distribution. Ruler top and bottom gradations in inches and centimeters, respectively.

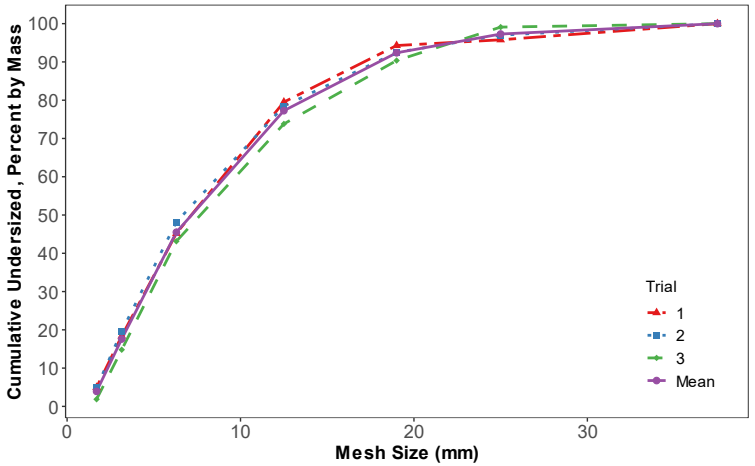

Figure 34. Particle size distribution of Chip #5, three repetitions and mean.

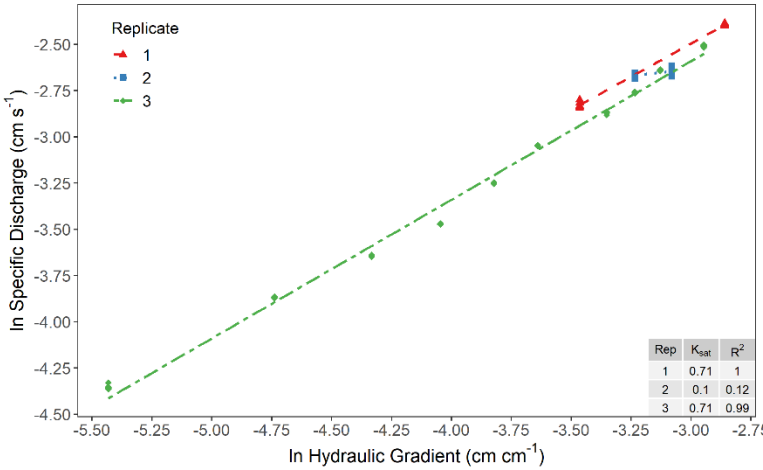

Figure 35. Saturated hydraulic conductivity calculation from regression of natural log corrected specific discharge and hydraulic gradient data for Chip #5. Viscosity adjusted K_{sat} values used for mean calculation shown in inset table.

Chip #6 – Cypress Mulch
Description: Bagged cypress mulch; mainly shredded, long and narrow particles, appeared to contain more fines than Chip 5
Source or Supplier: Prairie Gardens, Champaign, IL

Figure 36. Close-up photograph of Chip #6 with scale in centimeters.

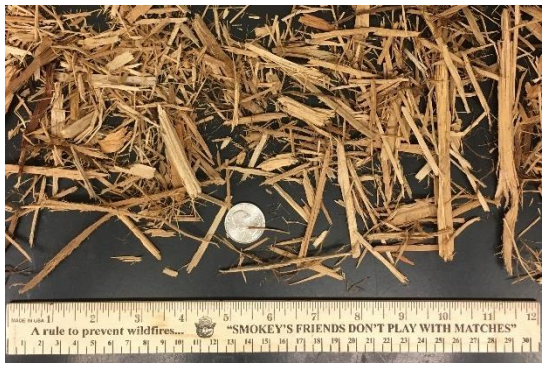

Figure 37. Large-scale photograph of Chip #6 depicting visual size distribution. Ruler top and bottom gradations in inches and centimeters, respectively.

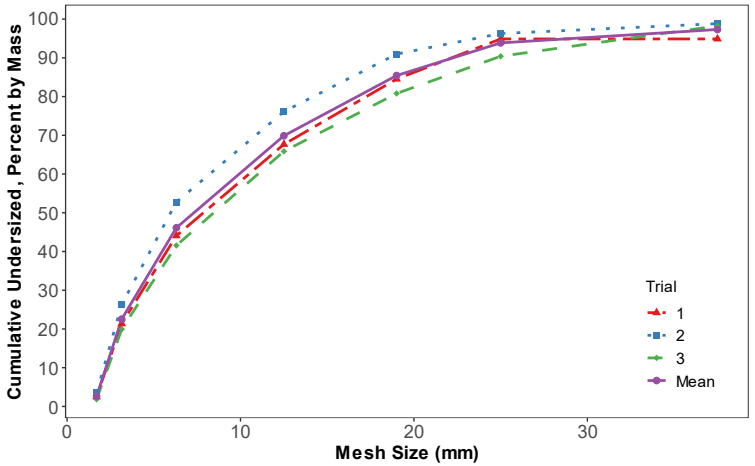

Figure 38. Particle size distribution of Chip #6, three repetitions and mean.

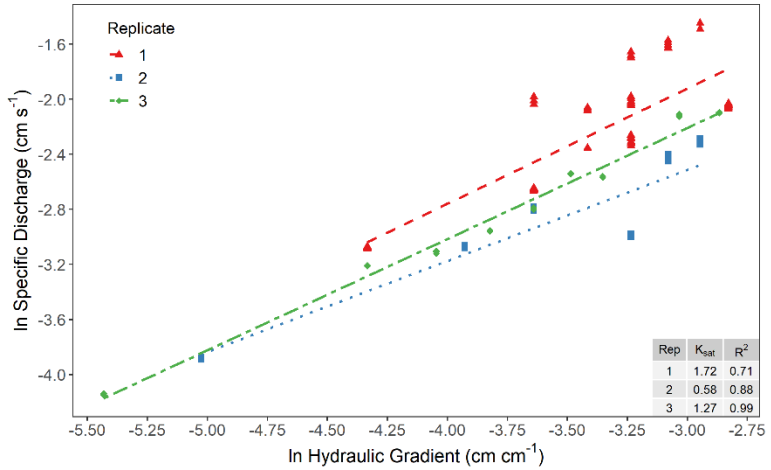

Figure 39. Saturated hydraulic conductivity calculation from regression of natural log corrected specific discharge and hydraulic gradient data for Chip #6. Viscosity adjusted K_{sat} values used for mean calculation shown in inset table.

Chip #7 – Pine Bark
Description: Bagged pine bark mulch; large, chunky pieces
Source or Supplier: Prairie Gardens, Champaign, IL

Figure 40. Close-up photograph of Chip #7 with scale in centimeters.

Figure 41. Large-scale photograph of Chip #7 depicting visual size distribution. Ruler top and bottom gradations in inches and centimeters, respectively.

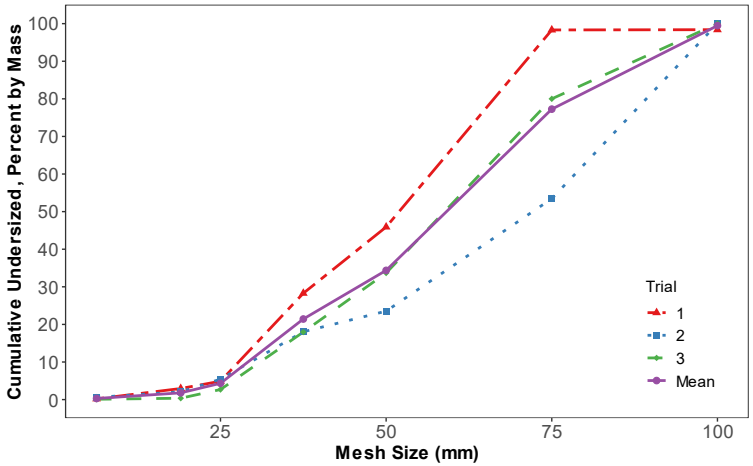

Figure 42. Particle size distribution of Chip #7, three repetitions and mean.

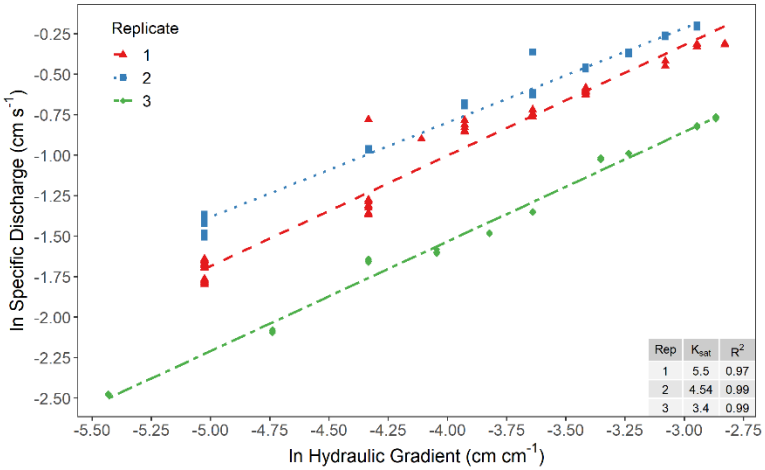

Figure 43. Saturated hydraulic conductivity calculation from regression of natural log corrected specific discharge and hydraulic gradient data for Chip #7. Viscosity adjusted K_{sat} values used for mean calculation shown in inset table.

Chip #8 – Shredded Cedar Mulch
Description: Bagged shredded cedar mulch; mainly small, fine pieces with minimal chipped particles
Source or Supplier: Menards, Champaign, IL

Figure 44. Close-up photograph of Chip #8 with scale in centimeters.

Figure 45. Large-scale photograph of Chip #8 depicting visual size distribution. Ruler top and bottom gradations in inches and centimeters, respectively.

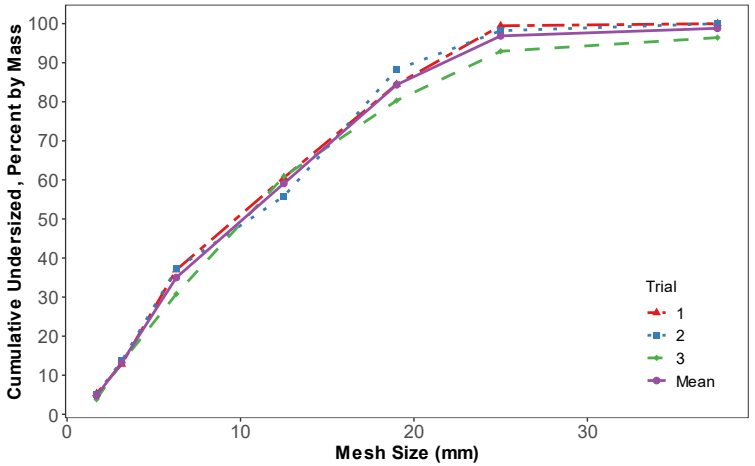

Figure 46. Particle size distribution of Chip #8, three repetitions and mean.

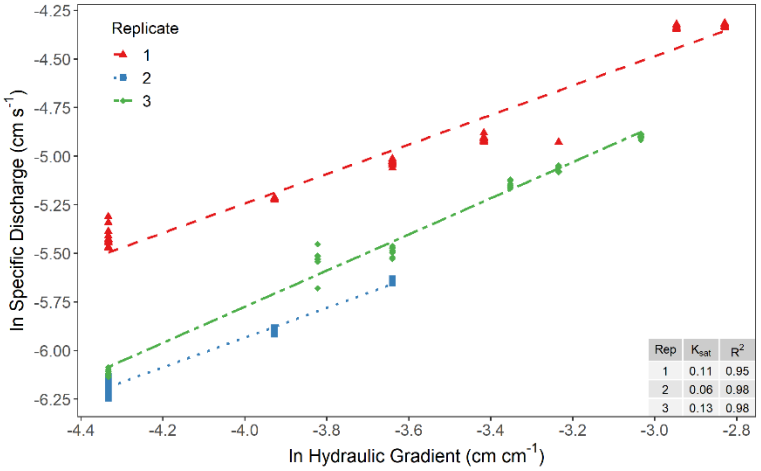

Figure 47. Saturated hydraulic conductivity calculation from regression of natural log corrected specific discharge and hydraulic gradient data for Chip #8. Viscosity adjusted K_{sat} values used for mean calculation shown in inset table.

Chip #9 – Dark Hardwood Mulch
Description: Bagged hardwood mulch; mix of shredded and chipped, mainly long and narrow particles, similar to Chip 6 but appeared to have more fines
Source or Supplier: Home Depot, Champaign, IL

Figure 48. Close-up photograph of Chip #9 with scale in centimeters.

Figure 49. Large-scale photograph of Chip #9 depicting visual size distribution. Ruler top and bottom gradations in inches and centimeters, respectively.

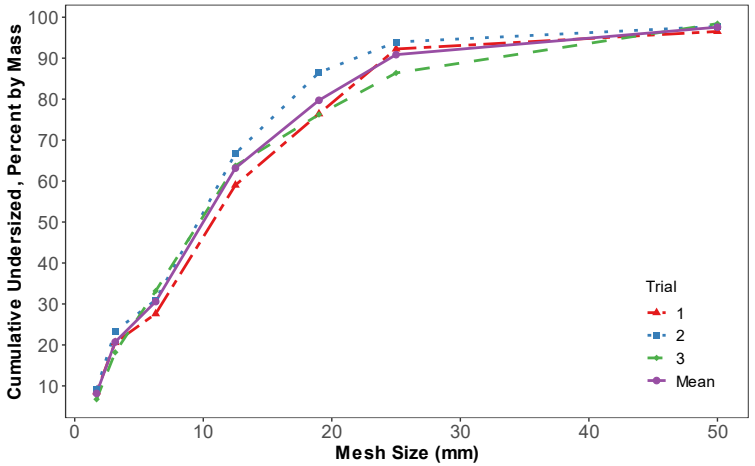

Figure 50. Particle size distribution of Chip #9, three repetitions and mean.

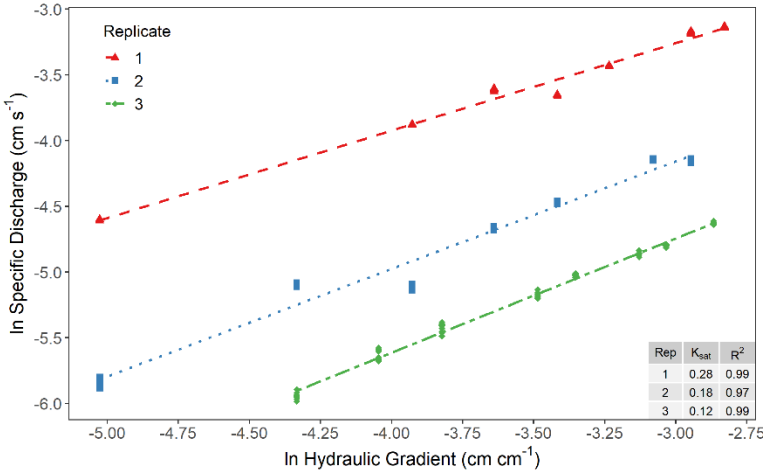

Figure 51. Saturated hydraulic conductivity calculation from regression of natural log corrected specific discharge and hydraulic gradient data for Chip #9. Viscosity adjusted K_{sat} values used for mean calculation shown in inset table.

Chip #10 – Decatur Municipal Woodchip
Description: Municipal tree debris mixed chips; heterogeneous mixture of sizes and shapes, included sticks, leaves, fines, and chunky pieces
Source or Supplier: City of Decatur, IL Forestry Department

Figure 52. Close-up photograph of Chip #10 with scale in centimeters.

Figure 53. Large-scale photograph of Chip #10 depicting visual size distribution. Ruler top and bottom gradations in inches and centimeters, respectively.

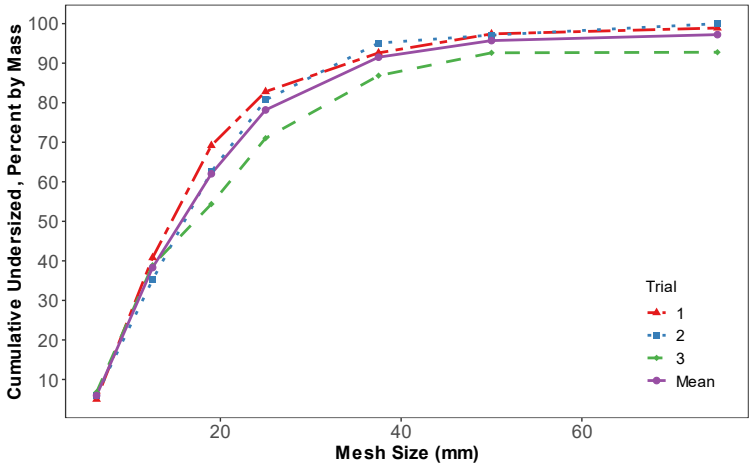

Figure 54. Particle size distribution of Chip #10, three repetitions and mean.

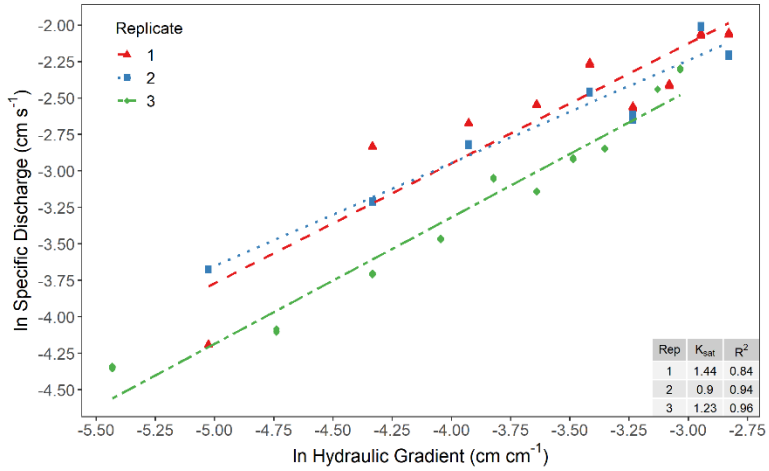

Figure 55. Saturated hydraulic conductivity calculation from regression of natural log corrected specific discharge and hydraulic gradient data for Chip #10. Viscosity adjusted K_{sat} values used for mean calculation shown in inset table.

Chip #11 – Premium Chipped Hardwood Mulch
Description: Composting facility mixed hardwood chips, mainly square-shaped particles, some fines; appeared more uniform than Chip #12
Source or Supplier: Landscape Recycling Center, Urbana, IL

Figure 56. Close-up photograph of Chip #11 with scale in centimeters.

Figure 57. Large-scale photograph of Chip #11 depicting visual size distribution. Ruler top and bottom gradations in inches and centimeters, respectively.

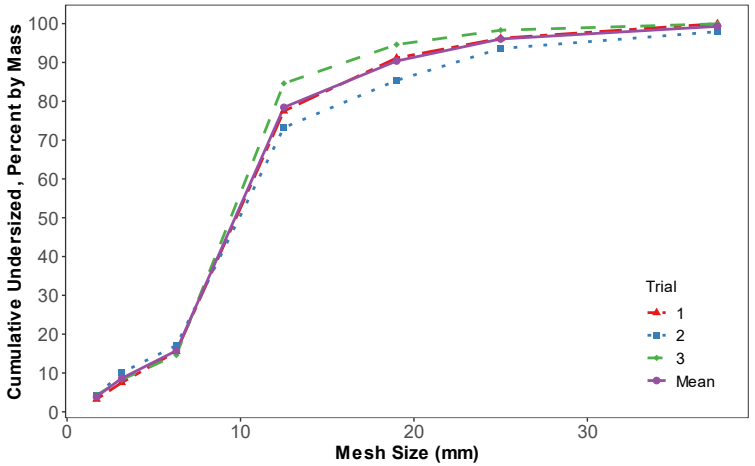

Figure 58. Particle size distribution of Chip #11, three repetitions and mean.

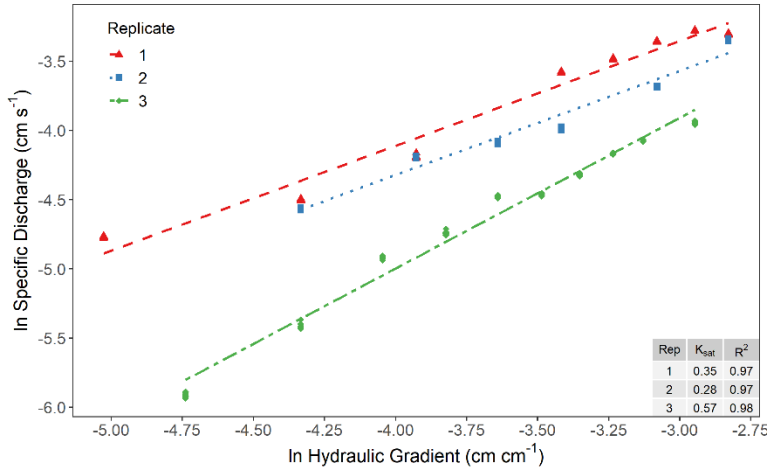

Figure 59. Saturated hydraulic conductivity calculation from regression of natural log corrected specific discharge and hydraulic gradient data for Chip #11. Viscosity adjusted K_{sat} values used for mean calculation shown in inset table.

Chip #12 – Select Chipped Hardwood Mulch
Description: Composting facility mixed hardwood chips, mainly square-shaped particles, appeared larger than Chip #11, included some small sticks, leaves, and chunky pieces
Source or Supplier: Landscape Recycling Center, Urbana, IL

Figure 60. Close-up photograph of Chip #12 with scale in centimeters.

Figure 61. Large-scale photograph of Chip #12 depicting visual size distribution. Ruler top and bottom gradations in inches and centimeters, respectively.

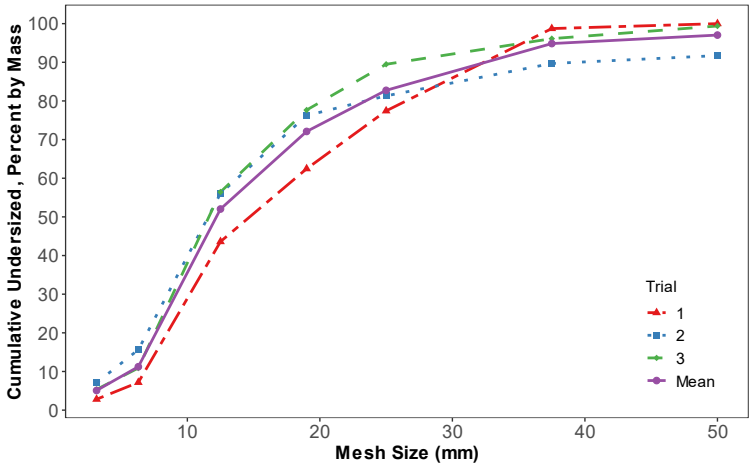

Figure 62. Particle size distribution of Chip #12, three repetitions and mean.

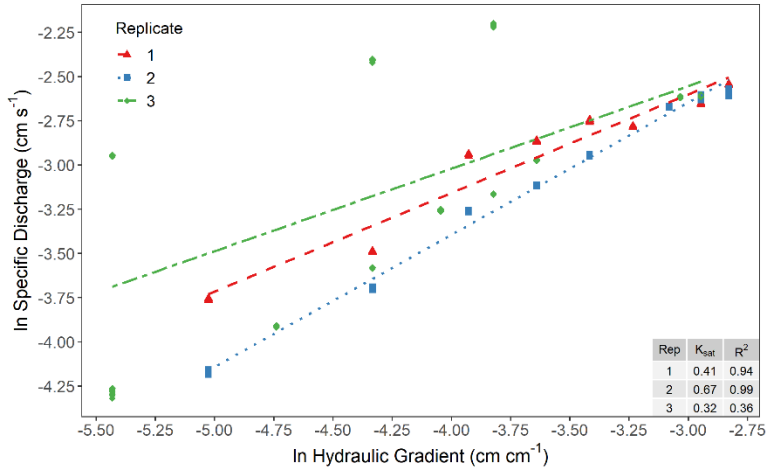

Figure 63. Saturated hydraulic conductivity calculation from regression of natural log corrected specific discharge and hydraulic gradient data for Chip #12. Viscosity adjusted K_{sat} values used for mean calculation shown in inset table.

Chip #13 – Private Farm Bioreactor Woodchips 1
Description: Maple-Oak (hardwood) Mixed Chips – meets NRCS bioreactor specifications; mainly square-shaped particles, appeared very uniform in size and shape
Source or Supplier: Xylem LTD, Cordova, IL

Figure 64. Close-up photograph of Chip #13 with scale in centimeters.

Figure 65. Large-scale photograph of Chip #13 depicting visual size distribution. Ruler top and bottom gradations in inches and centimeters, respectively.

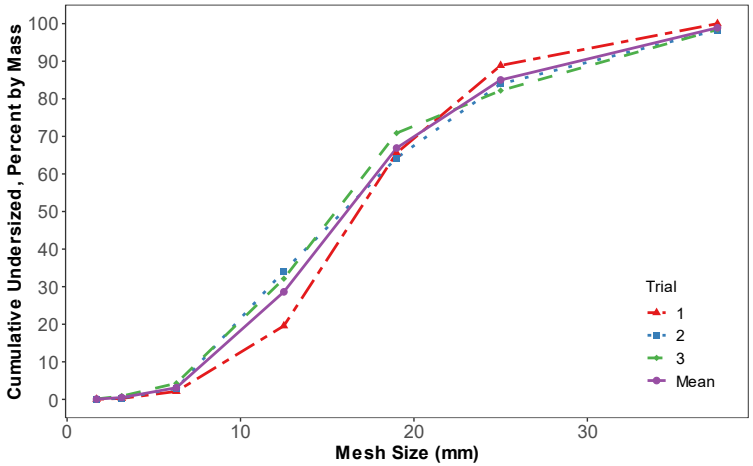

Figure 66. Particle size distribution of Chip #13, three repetitions and mean.

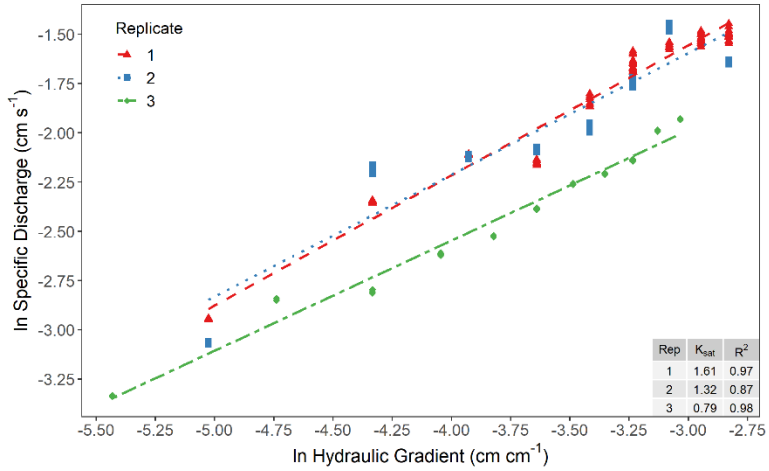

Figure 67. Saturated hydraulic conductivity calculation from regression of natural log corrected specific discharge and hydraulic gradient data for Chip #13. Viscosity adjusted K_{sat} values used for mean calculation shown in inset table.

Chip #14 – Hardwood Bioreactor Chips
Description: Mixed hardwood chips, generic mix supplier provides for bioreactors, mainly square-shaped particles, similar in appearance to Chip #13, but less uniform
Source or Supplier: Xylem LTD, Cordova, IL

Figure 68. Close-up photograph of Chip #14 with scale in centimeters.

Figure 69. Large-scale photograph of Chip #14 depicting visual size distribution. Ruler top and bottom gradations in inches and centimeters, respectively.

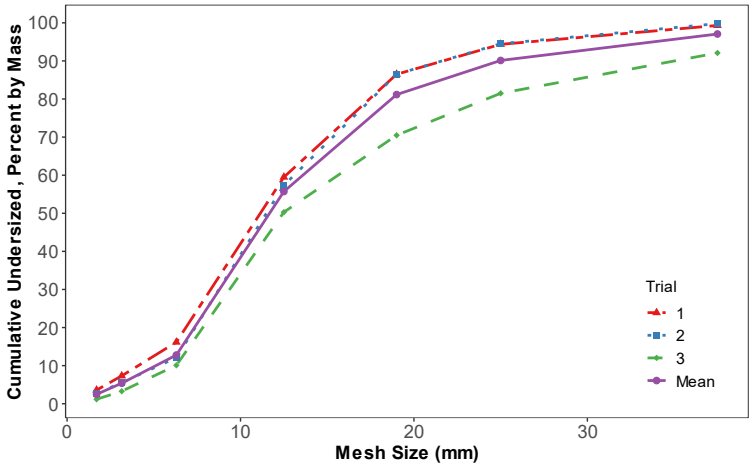

Figure 70. Particle size distribution of Chip #14, three repetitions and mean.

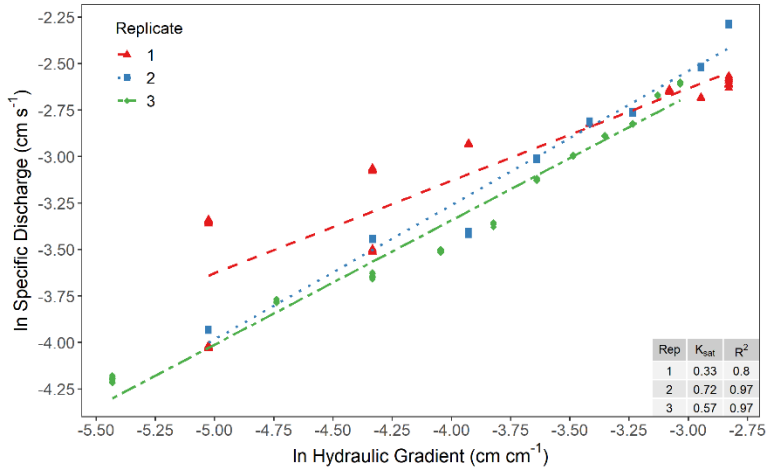

Figure 71. Saturated hydraulic conductivity calculation from regression of natural log corrected specific discharge and hydraulic gradient data for Chip #14. Viscosity adjusted K_{sat} values used for mean calculation shown in inset table.

Chip #15 – XylemMat Playground Chips
Description: Bagged hardwood playground chips, mainly small rectangular-shaped pieces, felt “mulchy”
Source or Supplier: Xylem LTD, Cordova, IL

Figure 72. Close-up photograph of Chip #15 with scale in centimeters.

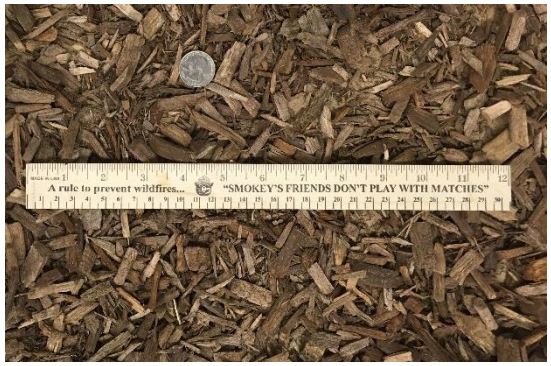

Figure 73. Large-scale photograph of Chip #15 depicting visual size distribution. Ruler top and bottom gradations in inches and centimeters, respectively.

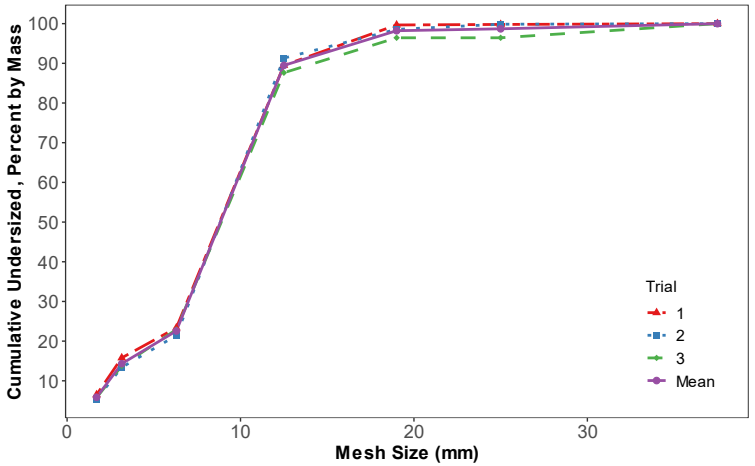

Figure 74. Particle size distribution of Chip #15, three repetitions and mean.

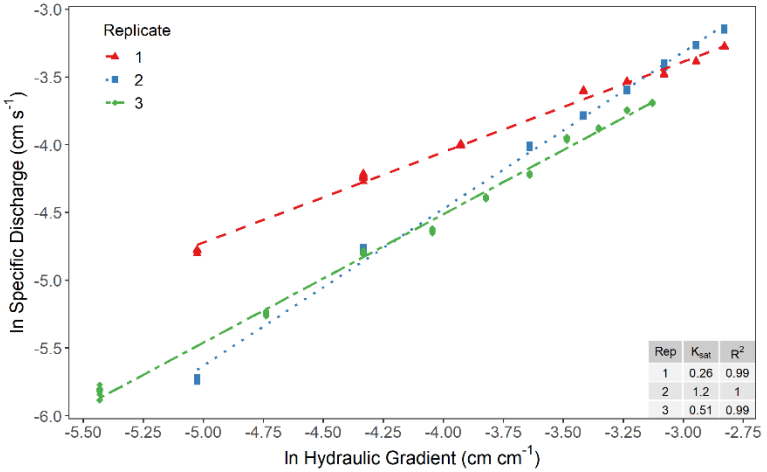

Figure 75. Saturated hydraulic conductivity calculation from regression of natural log corrected specific discharge and hydraulic gradient data for Chip #15. Viscosity adjusted K_{sat} values used for mean calculation shown in inset table.

Chip #16 – Davenport Municipal Chipped Mulch
Description: Municipal composting facility mixed oak chips, mainly square-shape particles
Source or Supplier: Davenport Compost Center, Davenport, IA

Figure 76. Close-up photograph of Chip #16 with scale in centimeters.

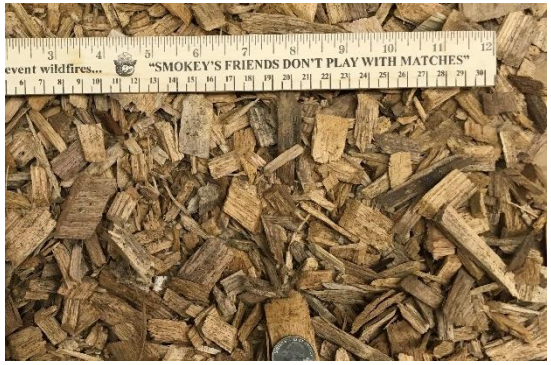

Figure 77. Large-scale photograph of Chip #16 depicting visual size distribution. Ruler top and bottom gradations in inches and centimeters, respectively.

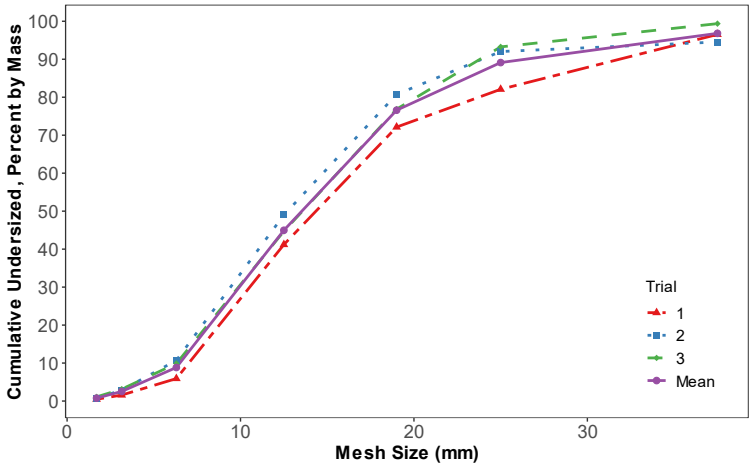

Figure 78. Particle size distribution of Chip #16, three repetitions and mean.

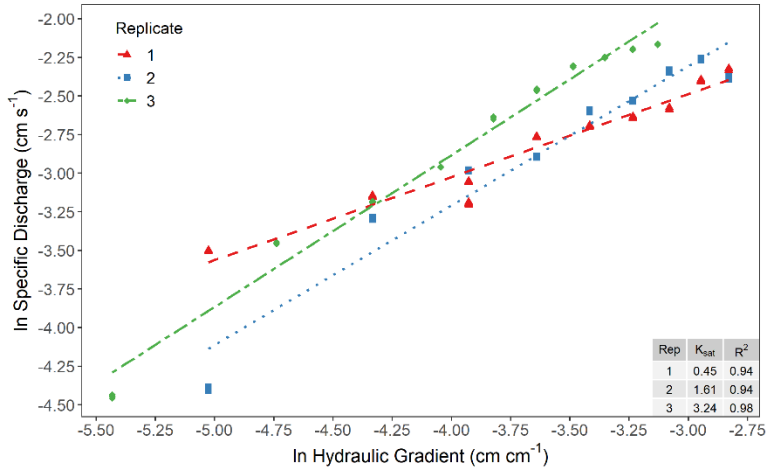

Figure 79. Saturated hydraulic conductivity calculation from regression of natural log corrected specific discharge and hydraulic gradient data for Chip #16. Viscosity adjusted K_{sat} values used for mean calculation shown in inset table.

Chip #17 – Cedar Rapids Municipal Woodchips
Description: Municipal tree debris mixed chips (derecho); smaller square-shaped particles mixed with other sizes and shapes; included some sticks, leaves, and fines
Source or Supplier: Cedar Rapids Solid Waste Agency, Cedar Rapids, IA

Figure 80. Close-up photograph of Chip #17 with scale in centimeters.

Figure 81. Large-scale photograph of Chip #17 depicting visual size distribution. Ruler top and bottom gradations in inches and centimeters, respectively.

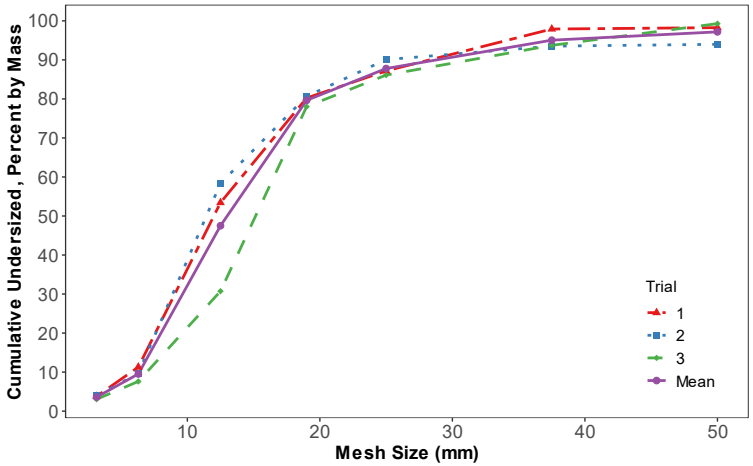

Figure 82. Particle size distribution of Chip #17, three repetitions and mean.

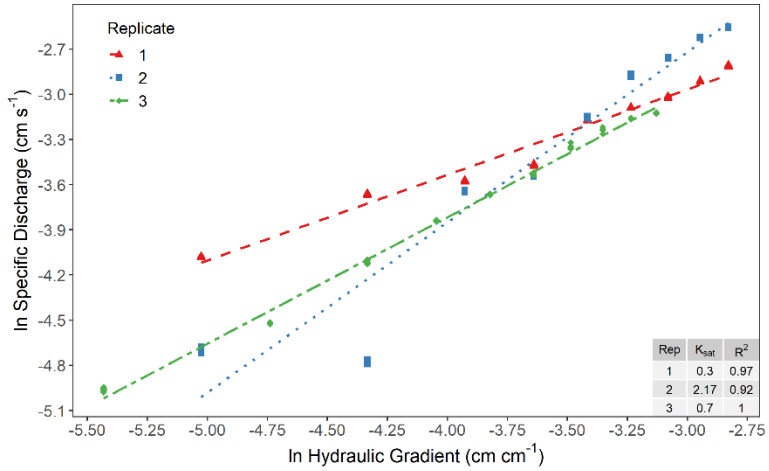

Figure 83. Saturated hydraulic conductivity calculation from regression of natural log corrected specific discharge and hydraulic gradient data for Chip #17. Viscosity adjusted K_{sat} values used for mean calculation shown in inset table.

Chip #18 – Fulton County Bioreactors Mixed Chips
Description: Bioreactor installation mixed chips, large square- and rectangular-shaped particles, included some chunky pieces
Source or Supplier: Corsaw Lumber, Smithfield, IL

Figure 84. Close-up photograph of Chip #18 with scale in centimeters.

Figure 85. Large-scale photograph of Chip #18 depicting visual size distribution. Ruler top and bottom gradations in inches and centimeters, respectively.

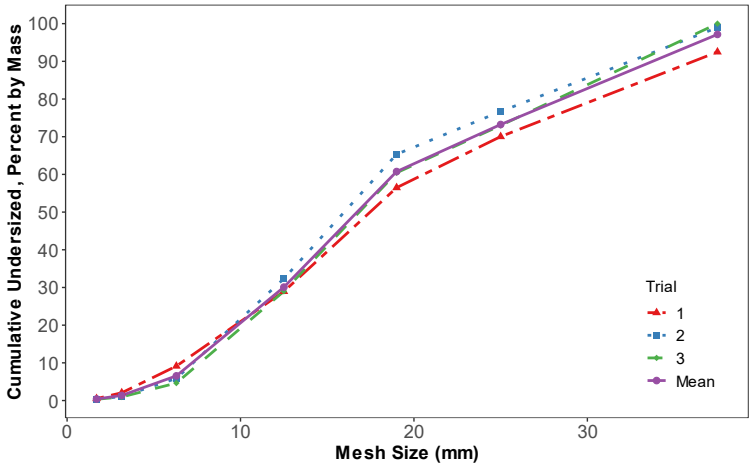

Figure 86. Particle size distribution of Chip #18, three repetitions and mean.

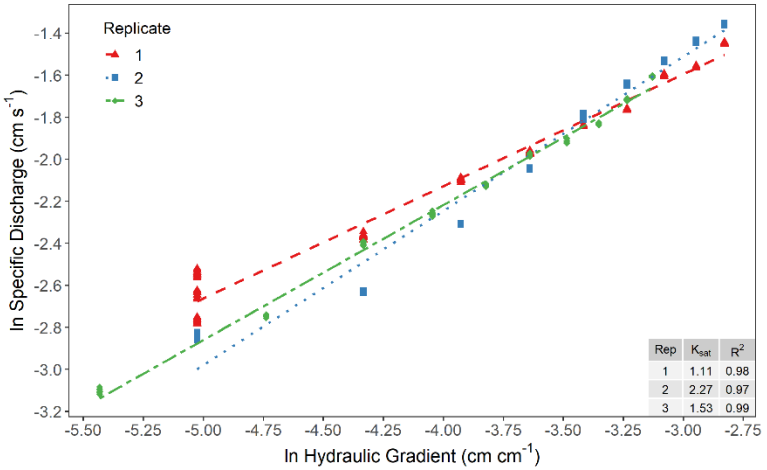

Figure 87. Saturated hydraulic conductivity calculation from regression of natural log corrected specific discharge and hydraulic gradient data for Chip #18. Viscosity adjusted K_{sat} values used for mean calculation shown in inset table.

Chip #19 – Large Chips Mulch
Description: Mixed softwood chips, large square-shaped particles, some rectangular-shape pieces, and some small pieces
Source or Supplier: Chips Groundcover, Holland, MI

Figure 88. Close-up photograph of Chip #19 with scale in centimeters.


Figure 89. Large-scale photograph of Chip #19 depicting visual size distribution. Ruler top and bottom gradations in inches and centimeters, respectively.

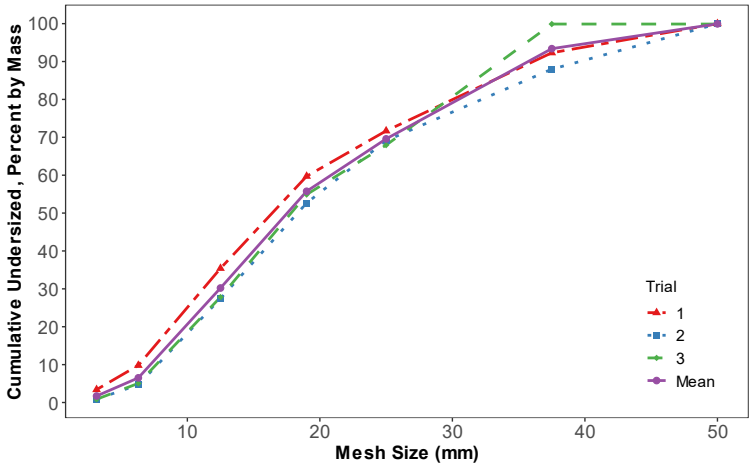

Figure 90. Particle size distribution of Chip #19, three repetitions and mean.

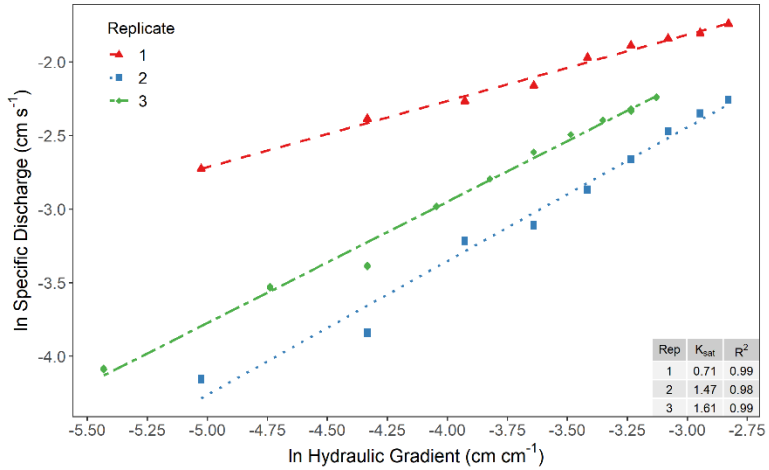

Figure 91. Saturated hydraulic conductivity calculation from regression of natural log corrected specific discharge and hydraulic gradient data for Chip #19. Viscosity adjusted K_{sat} values used for mean calculation shown in inset table.

Chip #20 – Natural Mulch
Description: Mixed shredded mulch; mainly long, narrow particles or short and narrow particles, some fines
Source or Supplier: Chips Groundcover, Holland, MI

Figure 92. Close-up photograph of Chip #20 with scale in centimeters.


Figure 93. Large-scale photograph of Chip #20 depicting visual size distribution. Ruler top and bottom gradations in inches and centimeters, respectively.

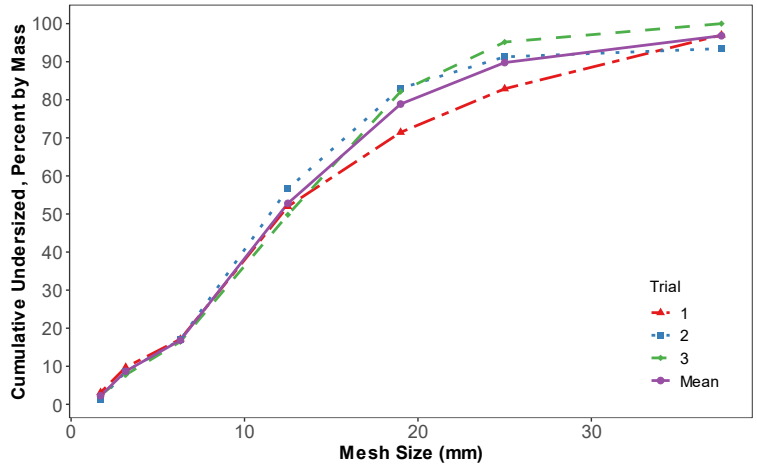

Figure 94. Particle size distribution of Chip #20, three repetitions and mean.

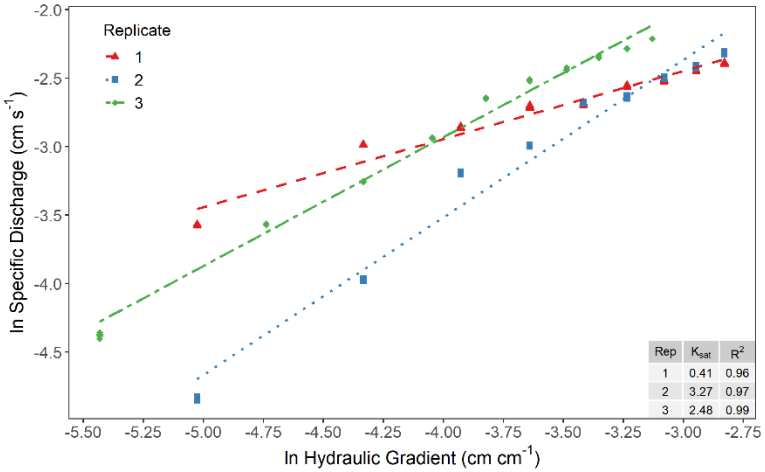

Figure 95. Saturated hydraulic conductivity calculation from regression of natural log corrected specific discharge and hydraulic gradient data for Chip #20. Viscosity adjusted K_{sat} values used for mean calculation shown in inset table.

Chip #21 – Private Farm Bioreactor Woodchips 2
Description: Mixed hardwood (primarily Hickory and Maple) chips – meets NRCS bioreactor specifications; mainly large square-shaped pieces, included some chunky pieces
Source or Supplier: Corsaw Lumber, Smithfield, IL

Figure 96. Close-up photograph of Chip #21 with scale in centimeters.


Figure 97. Large-scale photograph of Chip #21 depicting visual size distribution. Ruler top and bottom gradations in inches and centimeters, respectively.

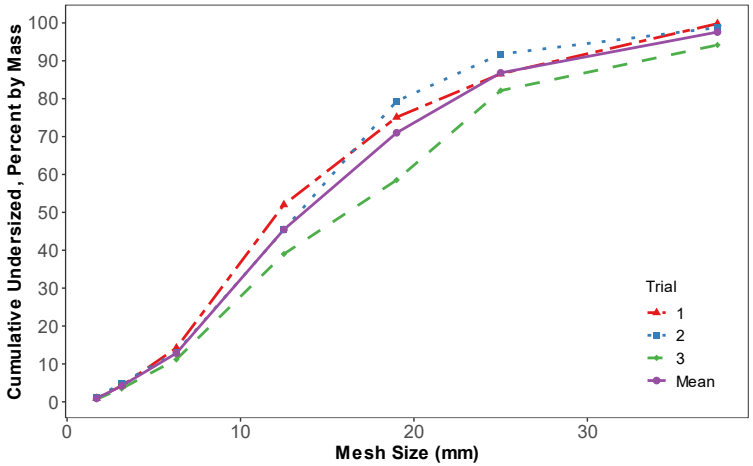

Figure 98. Particle size distribution of Chip #21, three repetitions and mean.

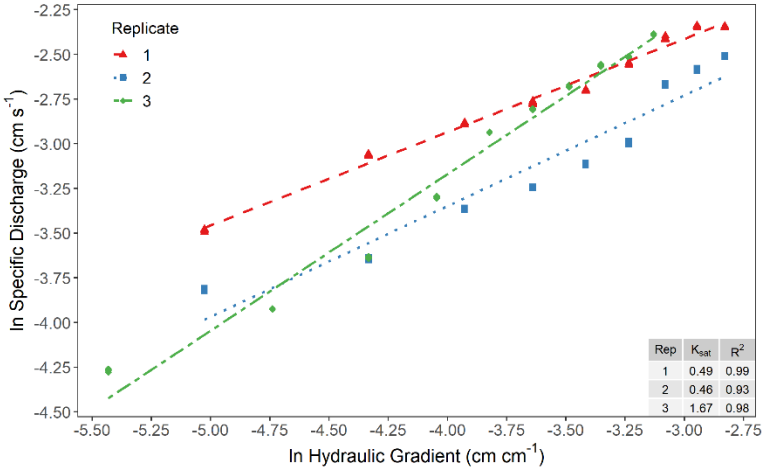

Figure 99. Saturated hydraulic conductivity calculation from regression of natural log corrected specific discharge and hydraulic gradient data for Chip #21. Viscosity adjusted K_{sat} values used for mean calculation shown in inset table.

APPENDIX B: REDUCED COMPACTION SPECIFIC DISCHARGE GRAPHS

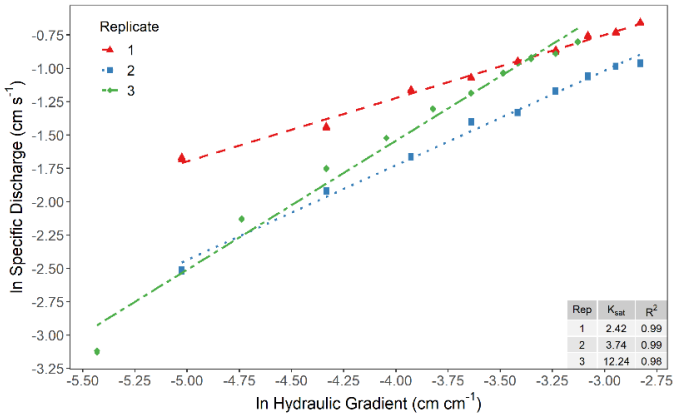

Figure 100. Saturated hydraulic conductivity calculation from regression of natural log corrected specific discharge and hydraulic gradient data for Chip #5 at low compaction (0 tamps). Viscosity adjusted K_{sat} values used for mean calculation shown in inset table

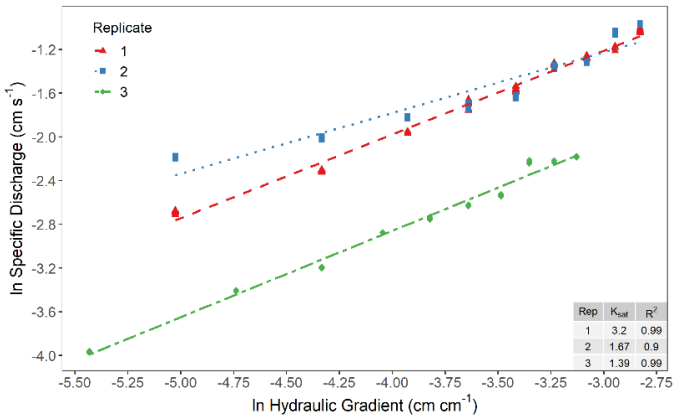

Figure 101. Saturated hydraulic conductivity calculation from regression of natural log corrected specific discharge and hydraulic gradient data for Chip #5 at medium compaction (10 tamps). Viscosity adjusted K_{sat} values used for mean calculation shown in inset table

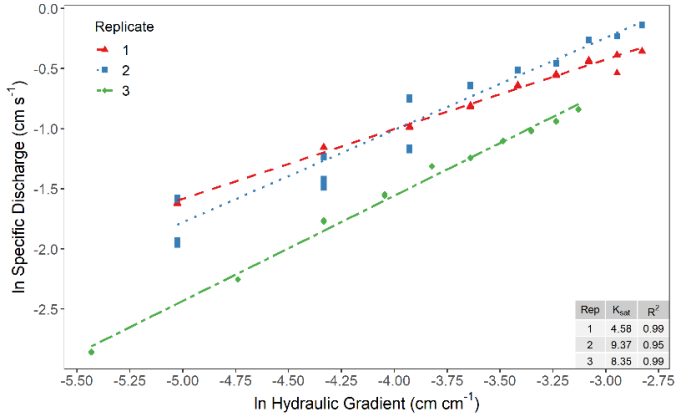

Figure 102. Saturated hydraulic conductivity calculation from regression of natural log corrected specific discharge and hydraulic gradient data for Chip #13 at low compaction (0 tamps). Viscosity adjusted K_{sat} values used for mean calculation shown in inset table.

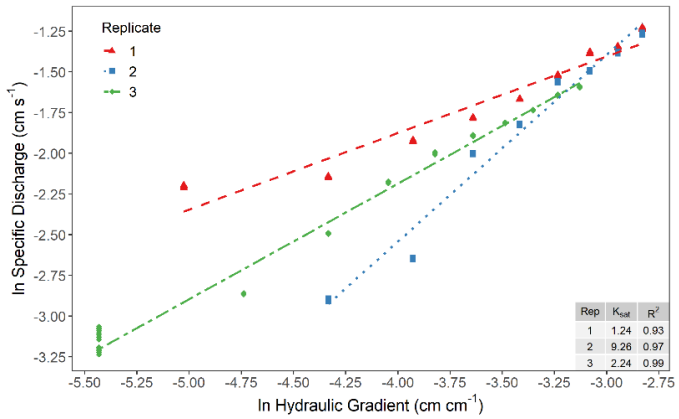

Figure 103. Saturated hydraulic conductivity calculation from regression of natural log corrected specific discharge and hydraulic gradient data for Chip #13 at medium compaction (10 tamps). Viscosity adjusted K_{sat} values used for mean calculation shown in inset table.

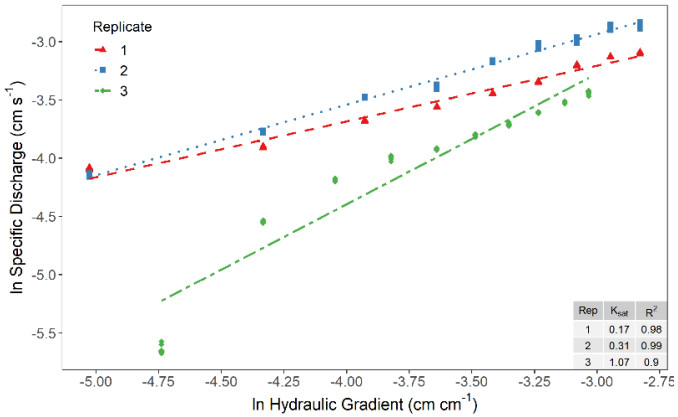

Figure 104. Saturated hydraulic conductivity calculation from regression of natural log corrected specific discharge and hydraulic gradient data for Chip #15 at low compaction (0 tamps). Viscosity adjusted K_{sat} values used for mean calculation shown in inset table.

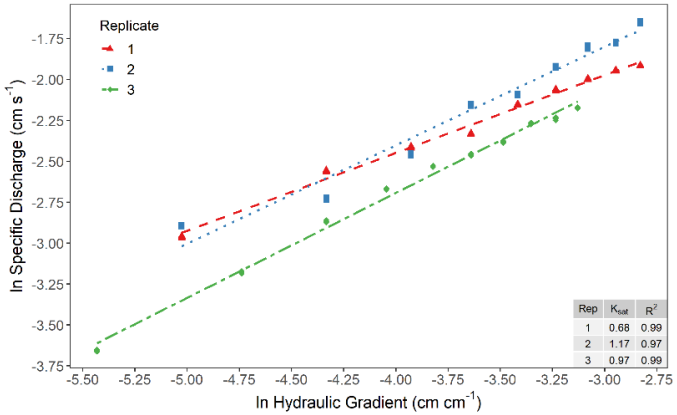

Figure 105. Saturated hydraulic conductivity calculation from regression of natural log corrected specific discharge and hydraulic gradient data for Chip #15 at medium compaction (10 tamps). Viscosity adjusted K_{sat} values used for mean calculation shown in inset table.

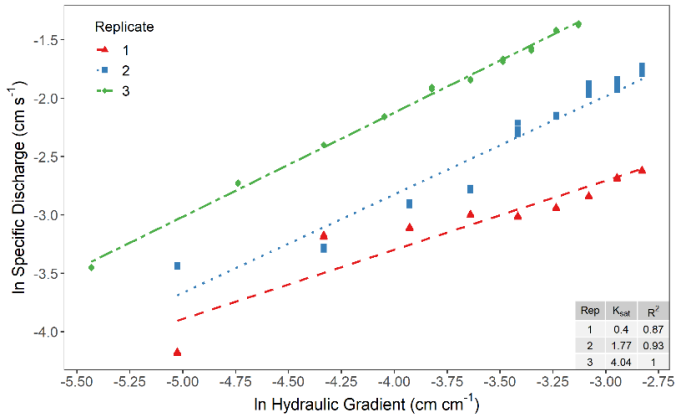

Figure 106. Saturated hydraulic conductivity calculation from regression of natural log corrected specific discharge and hydraulic gradient data for Chip #21 at low compaction (0 tamps). Viscosity adjusted K_{sat} values used for mean calculation shown in inset table.

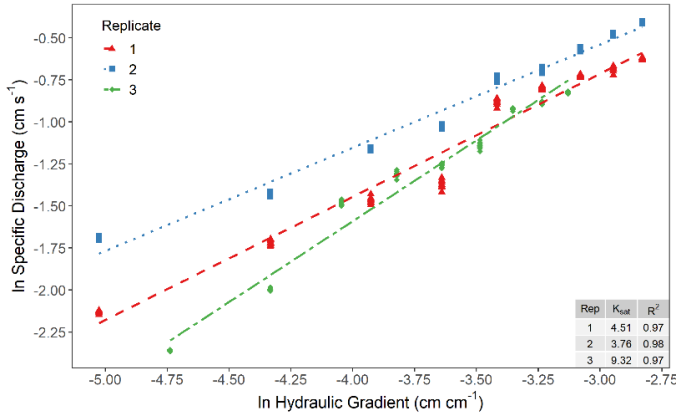

Figure 107. Saturated hydraulic conductivity calculation from regression of natural log corrected specific discharge and hydraulic gradient data for Chip #21 at medium compaction (10 tamps). Viscosity adjusted K_{sat} values used for mean calculation shown in inset table.

APPENDIX C: WOODCHIP SOURCE LOCATIONS

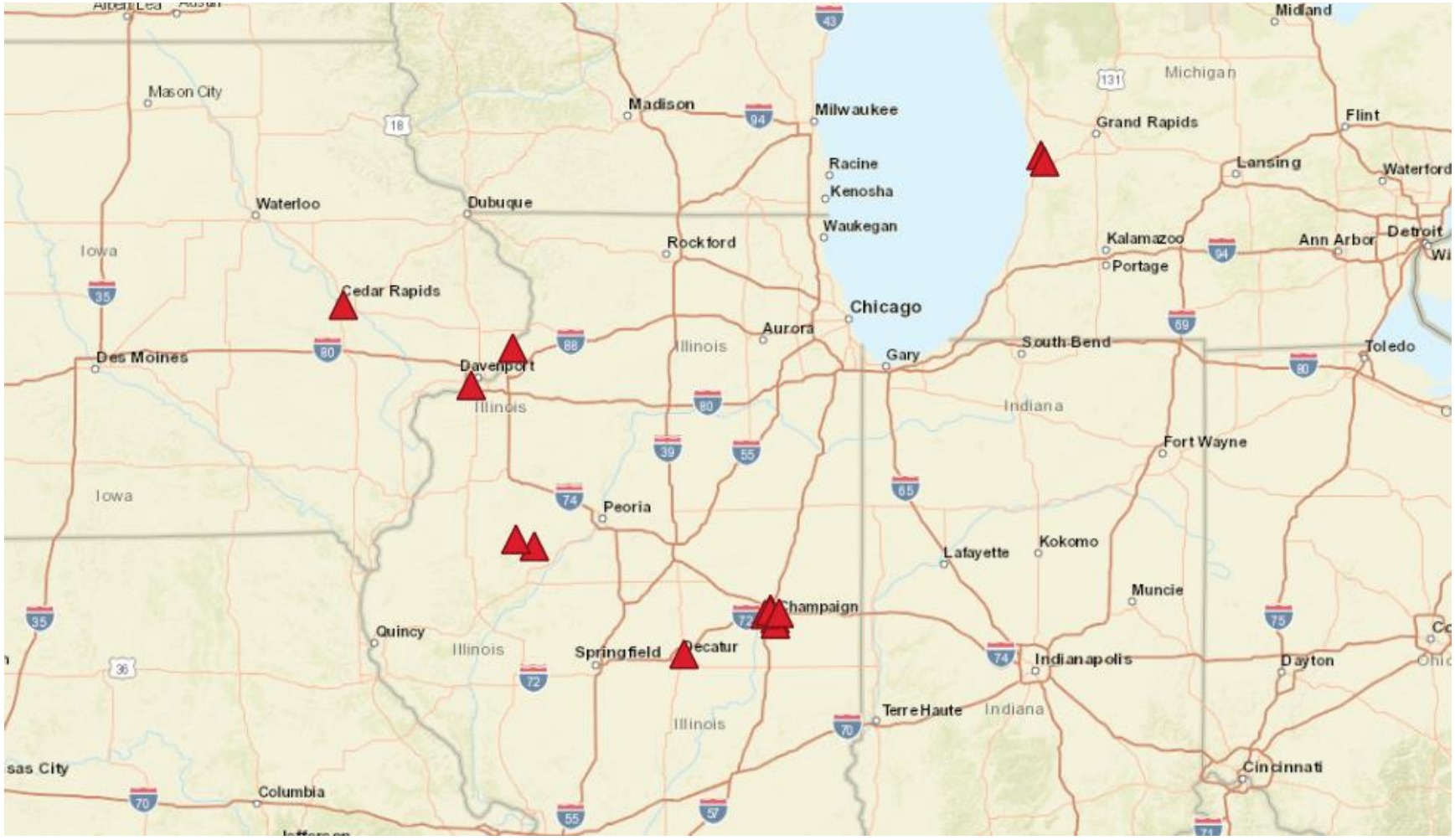

Figure 108. Map of source locations for twenty-one woodchip types collected across the U.S. Midwest region.